New Journal of Chemistry

Supporting Information

Gold/iron oxide coreshell nanostructures for oxidation of indoles and synthesis of uracil-derived spirooxindoles

Shivanee B. Gohain,[a] Purna K. Boruah,[b] Manash R. Das[b] and Ashim J. Thakur*[a]

[a]*Dept. Of Chemical Sciences, Tezpur University, Napaam 784028, Assam, INDIA*; [b]*Advanced Materials Group, Materials Sciences and Technology Division, CSIR-North East Institute of Science and Technology (NEIST), Jorhat 785006, Assam, India*

Graphical abstract:

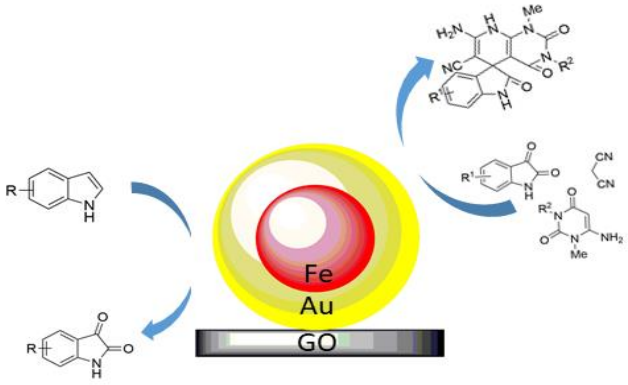

Synthesis of isatins and uracil based spirooxindoles catalysed by Au/Fe_3O_4 core shell nanoparticles under mild condition and low reaction times.

List of contents

(1) General Experimental Methods

All chemicals were purchased from Sigma-Aldrich, Merck, Alfa Aesar and Loba chemical, and used without any further purification. $HAuCl_4.3H_2O$ (99% purity) and $FeSO_4.7H_2O$ (99% purity) were procured from Sigma-Aldrich. Deionized water was used for the preparation of catalyst. Graphite (98% purity) was purchased from Loba Chemie. The solvents used in different reactions were purchased from E-Merck. Melting points were determined in a Büchi 504 apparatus. ^1H and ^{13}C NMR spectra were recorded in a 400 MHz NMR spectrophotometer (JEOL, JNM ECS) using tetramethylsilane (TMS) as the internal standard and coupling constants are expressed in Hertz. Visualization of organic products was accomplished with UV lamp or I_2 stain. The reactions were monitored by thin-layer chromatography using aluminium sheets with silica gel 60 F_{254} (Merck).

(2) Preparation of catalysts

Preparation of GO.

GO was prepared by oxidizing graphite according to the modified Hummer's method.[1,2]

Preparation of Fe_3O_4/AuNPs

Fe_3O_4 NPs were prepared by the reduction of Fe^{2+} with $NaBH_4$. A total of 0.2 g (1.3 mmol) of $FeSO_4$ was added to 0.1 g (2.8 mmol) of $NaBH_4$ and the mixture was stirred at room temperature for 1 h. A dark powder was obtained, to which 100 mL of distilled water was added. To create Au shell on the Fe core, 0.05 g (0.16 mmol) of $HAuCl_4$ was added to the solution of $FeSO_4$ and $NaBH_4$. The resulting black solution was heated to 100 $^{\circ}$C. A total of 0.4 g (1.5 mmol) of the trisodium citrate solution in 10 mL of water was immediately added to the solution, and it was left stirring (~1400 rpm) at room temperature overnight. A black colloidal solution was obtained. The sample was dried in a vacuum for elemental analysis.

Preparation of Fe_3O_4/Au NPs-rGO.

Fe-Au NPs were synthesized according to the above-mentioned method. The mixture of 80 mL aqueous solution of Fe NPs and 1g of GO was stirred at room temperature overnight, and the product was dried at 40 ˚C overnight.

(3) Characterization of the catalysts

The UV-visible spectra of Au nano catalysts were recorded on UV-Visible spectrophotometer (Hitachi, U-2001, Shimadzu, UV-2550 Model Cary 100 Bio). Field mission transmission electron microscopy (FETEM) images and energy dispersive Xray (EDX) analyses of nanocatalysts were carried out on JEOL (Model 2100F) and Tecnai G2 20 S-Twin (200kV) TEM. X-ray diffraction (XRD) measurement was performed on Bruker AXS, model D8 Focus. Scanning electron microscopy (SEM) and electron-dispersive X-ray spectroscopy (EDS or EDX) mapping were done in JEOL, Japan, model JSM 6390LV. The high-resolution X-ray photoelectron spectroscopy (XPS) measurements using a Thermo-Scientific ESCALAB Xi+ spectrometer with a monochromatic Al Kα X-ray source (1486.6 eV).

(4) General Synthetic Procedures

(A) General Procedure for synthesis of 2,3-indolinones (isatins)

For a typical reaction (Scheme 1), nanocatalyst and solvent (3 ml) were added into the reaction vessel and then followed by indole (0.5 mmol). The reaction vessel was sealed and stirred at room temperature for 6 h. After its completion, ethyl acetate (3x10 mL) was added to it and then centrifuged at 3,500 rpm to recover the nano catalyst. Having done this, the reaction mixture was washed with water and brine, dried over Na_2SO_4, concentrated in a rotary evaporator and finally the crude product was purified by column chromatography (30% ethyl acetate: hexane as an eluent).

(B) General Procedure for synthesis of spiroxindoles

For a typical reaction (Scheme 2), nanocatalyst and solvent (3 ml) were added into the reaction vessel and then followed by indole (0.5 mmol), malononitrile (0.5 mmol) and

6-amino-1-methyluracil (0.5 mmol). The reaction vessel was sealed and stirred at room temperature for 5 min. After its completion, methanol (1x10 mL) was added to it and then centrifuged at 3,500 rpm to recover the nano catalyst. Having done this, the reaction mixture filtered through Whatmann filter paper No. 1 and the products were recrystallised.

(5) Recycling potentials of nanocatalysts

After carrying out the experiment, ethyl acetate was added, and the reaction mixture was centrifuged to pellet out the Fe_3O_4/Au NPs-rGO nanocomposite. The particles were then extracted by simple centrifugation (3,000 rpm) and washed with hot ethanol (3x10 mL) to remove all the organic impurities. Finally, it was decanted and dried in vacuum. The recovered nanocatalyst was used directly in the next cycle. The Fe_3O_4/Au NPs-rGO nanocomposite was found to be equally effective up to 3rd and 4th cycle (Fig. S12, ESI) for isatin and spirooxindole synthesis respectively, and after that the product yield slightly decreases.

(6) List of figures

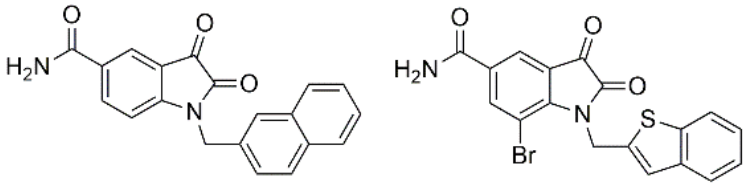

Figure S1. Examples of isatin based moieties in the potential drugs designed inhibitors for SARS-CoV-2

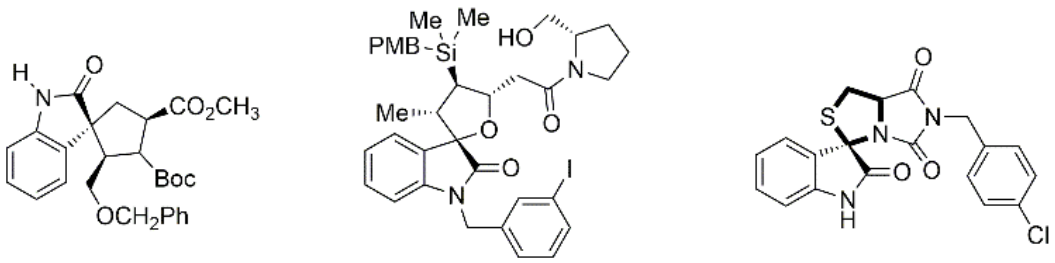

Figure S2. Examples of spirooxindole derived compounds with anti-cancer properties

Figure S3. (a) Image of Fe_3O_4/Au NPs and Image of Fe_3O_4/Au NPs-rGO

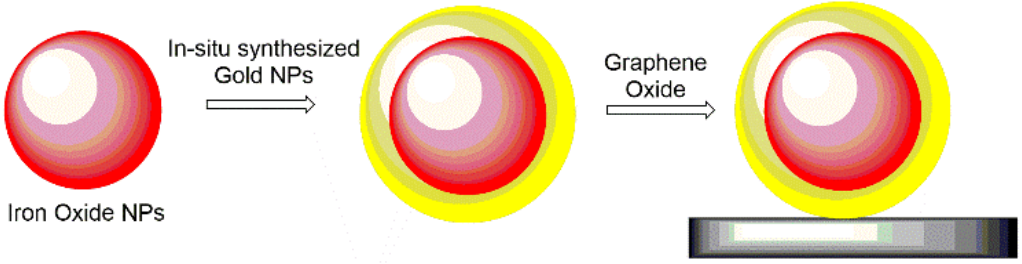

Figure S4. Schematic representation of formation of gold (yellow) coated iron oxide (red) NPs and gold coated iron oxide NPs supported on *in-situ* synthesized reduced graphene oxide (black)

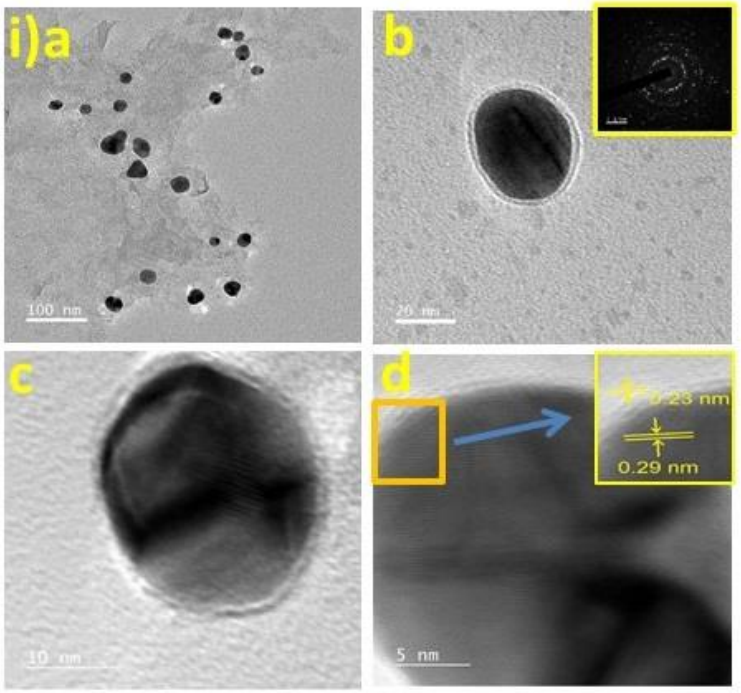

Figure S5(i). FETEM images of Fe_3O_4/Au NPs (inset in (b) shows SAED pattern; inset in (d) shows lattice fringe pattern of Au and Fe_3O_4 NPs

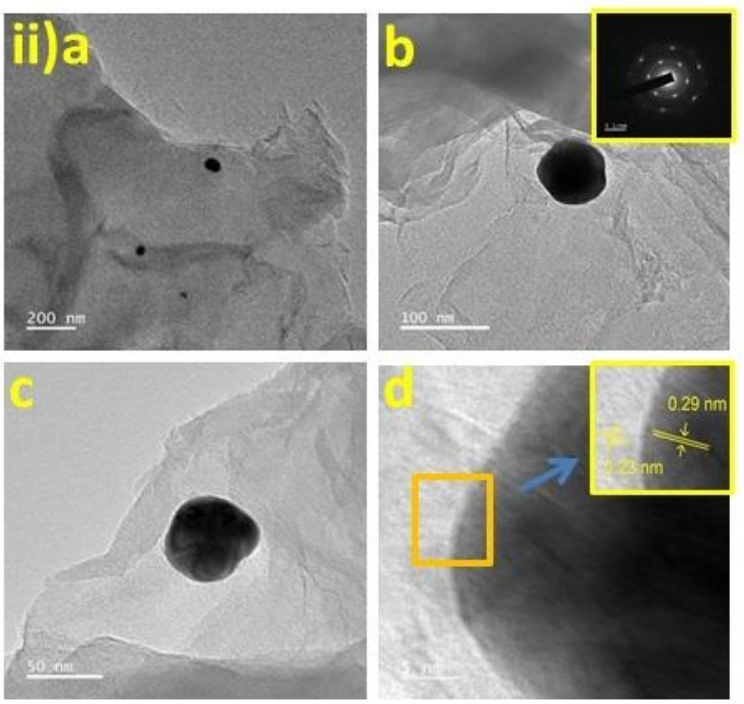

Figure S5(ii). FETEM images of Fe_3O_4/Au NPs-rGO (inset in (b) shows SAED pattern; inset in (d) shows lattice fringe pattern of Au and Fe_3O_4 NPs)

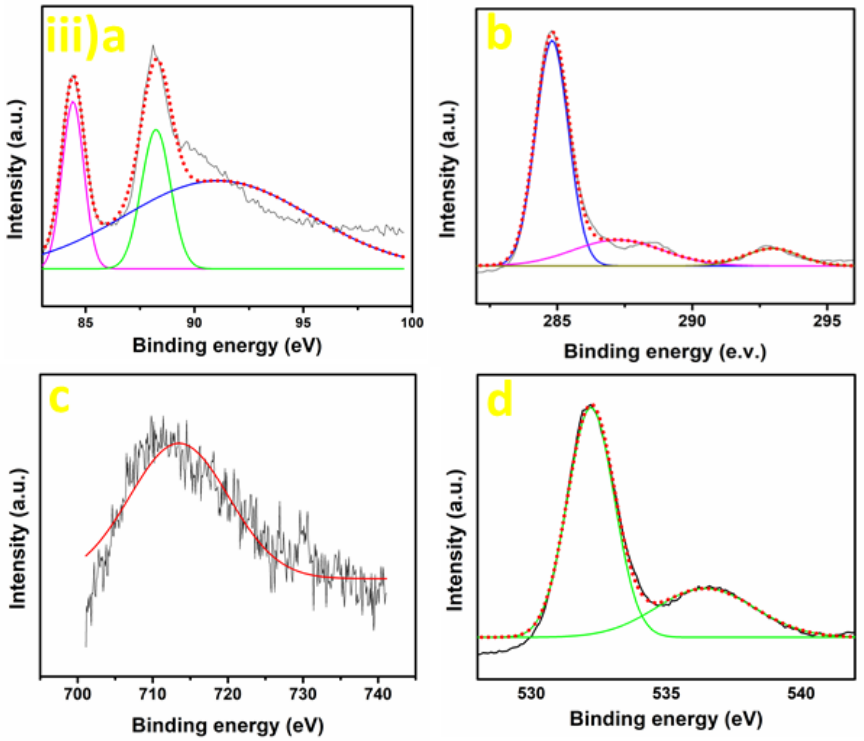

Figure S5(iii). XPS high resolution spectra of (a) Au 4*f* (b) C 1s (c) Fe 2*p* and (d) O 1s of Fe_3O_4/Au NPs

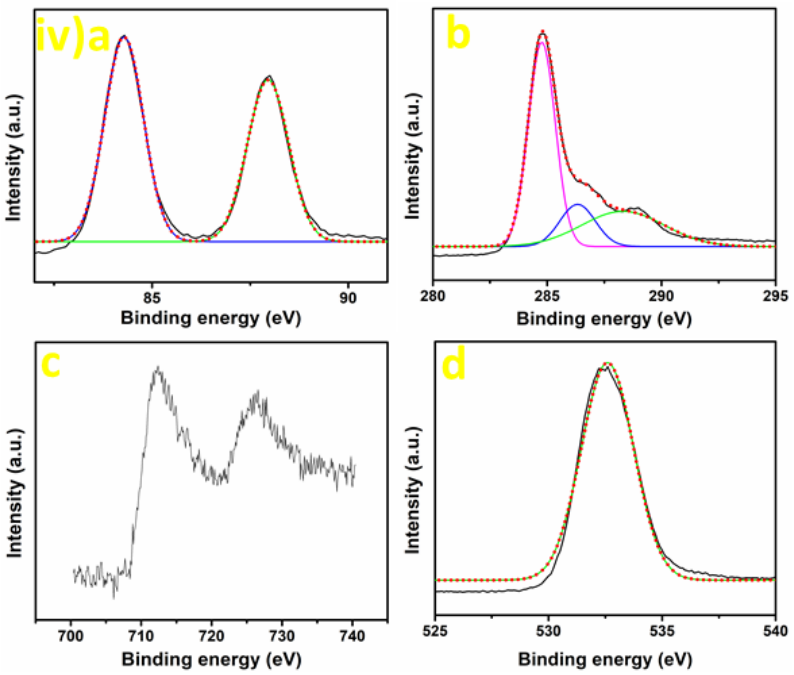

Figure S5(iv). XPS high-resolution spectra of (a) Au 4*f* (b) C 1s (c) Fe 2*p* and (d) O 1s of Fe_3O_4/Au NPs-rGO.

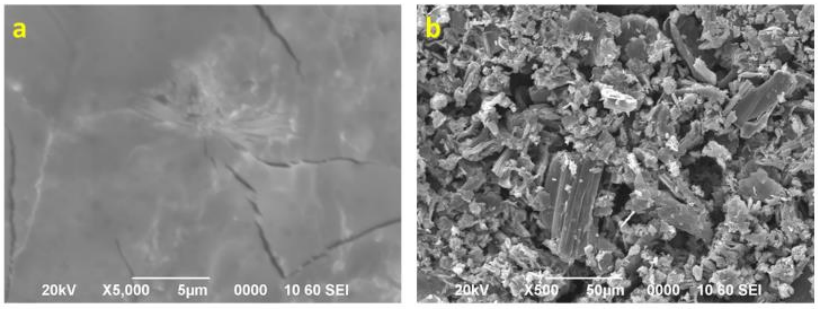

Figure S6. SEM images of the (a) Fe_3O_4/Au NPs and (b) Fe_3O_4/Au NPs-rGO

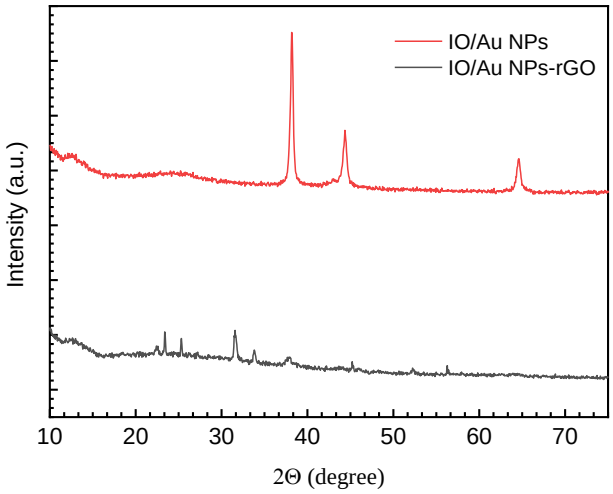

Figure S7. XRD pattern of Fe_3O_4/Au NPs (red), Fe_3O_4/Au NPs-rGO (blue)

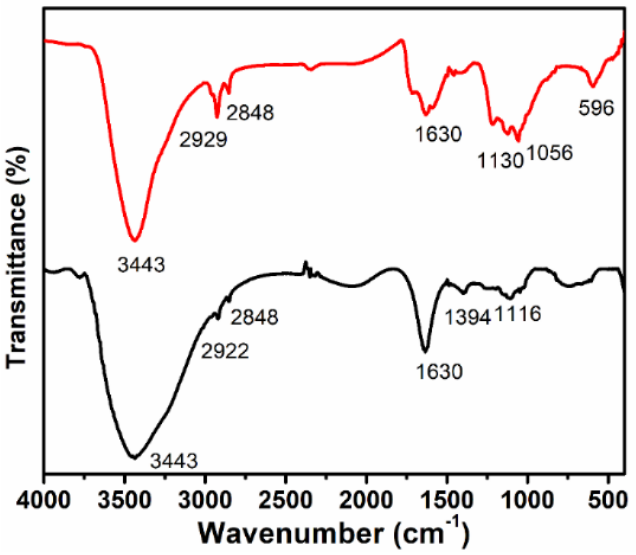

Figure S8. FTIR spectra of Fe_3O_4/Au NPs (black) and Fe_3O_4/Au NPs-rGO (red)

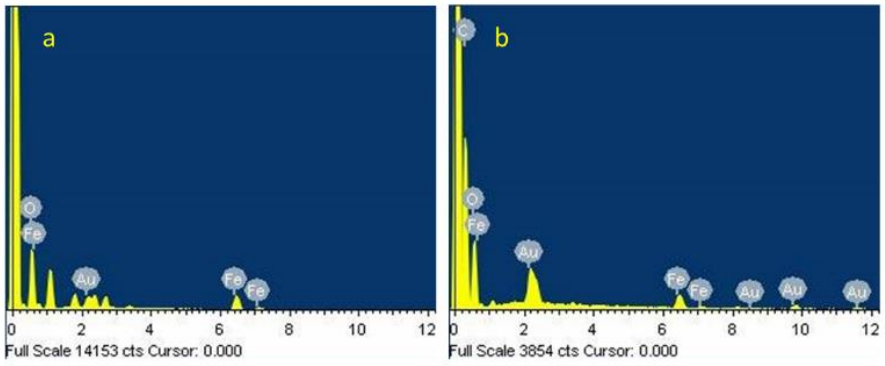

Figure S9. EDX spectra of (a) Fe_3O_4/Au NPs and (b) Fe_3O_4/Au NPs-rGO

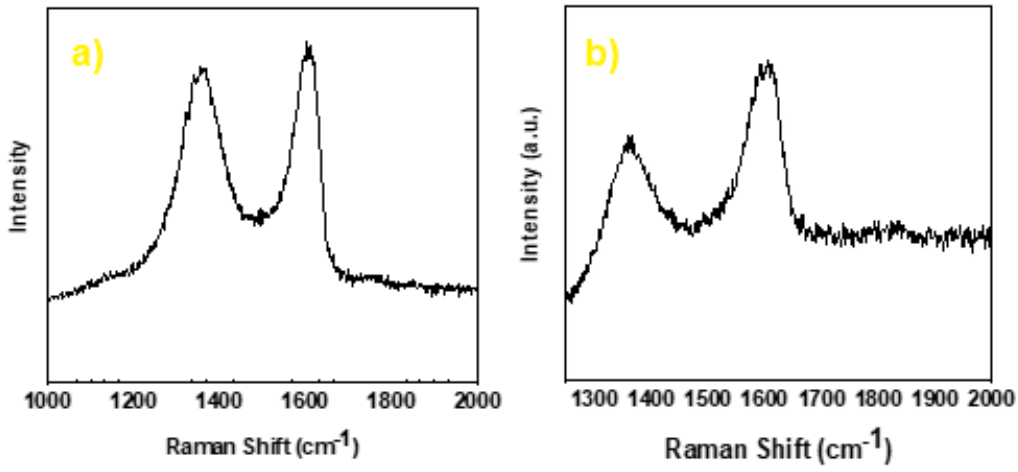

Figure S10. Raman spectra of (a) GO and (b) Fe_3O_4/Au NPs-rGO

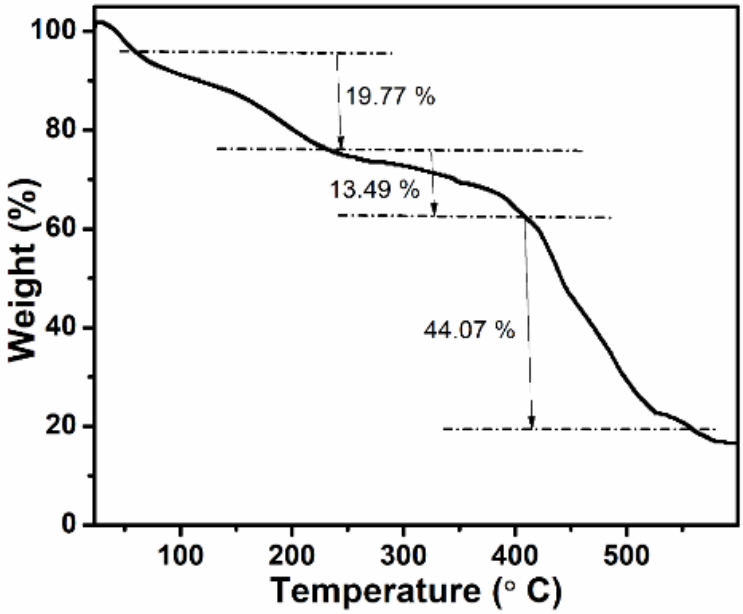

Figure S11. TGA curve of Fe_3O_4/Au NPs-rGO

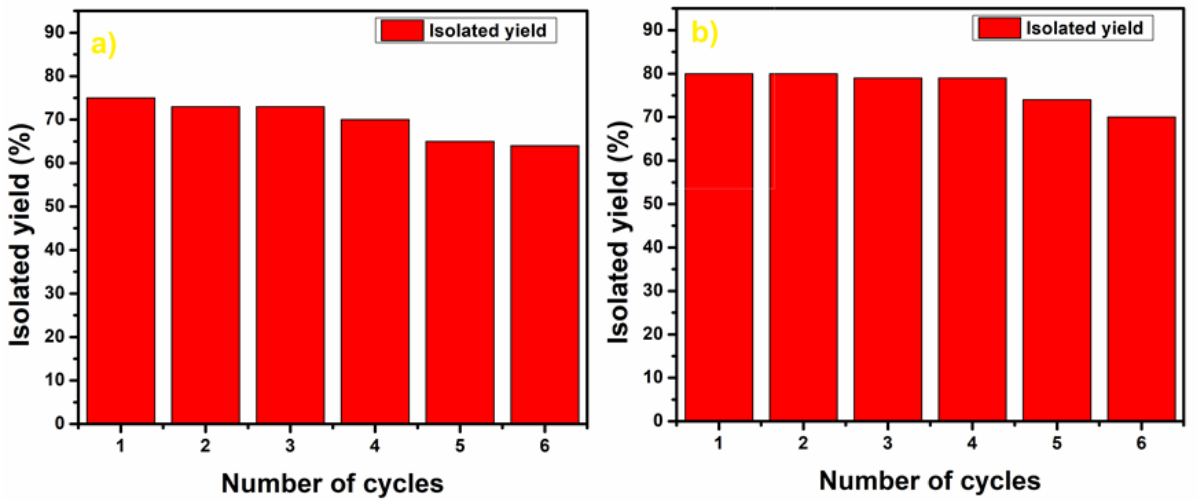

Figure S12. Catalyst recyclability chart of Fe_3O_4/Au NPs-rGO for a) isatin and b) spirooxindole synthesis

(7) List of tables

Table S1. Observed infrared band positions for Fe_3O_4/Au NPs and Fe_3O_4/Au NPs-rGO

Peak assignments	Fe_3O_4/Au NPs	Peak assignments	Fe_3O_4/Au NPs-rGO
Hydroxyl stretch	3443	Hydroxyl stretch	3443
CH of citrate	2922	CH_2 stretching of alcohol groups of GO	2929
CH of citrate	2848	CH_2 stretching of alcohol groups of GO	2848
symmetric C=O stretching from the COOH group of citrate	1630	C=C stretches from unoxidized graphitic domain	1630
asymmetric stretching of C-O from COOH group of citrate	1349		
	1116	C-O stretching vibrations of C-O-C stretching of GO	1130
		to C-O stretching vibrations of C-O stretching of G	1056
		Fe–O stretching vibrational mode of Fe_3O_4	596

Table S2. Atomic percentage of different elements in the nanomaterials

(Nano Au)	Fe	O	Au	C
Fe_3O_4/Au NPs	6.53	92.05	1.43	-
Fe_3O_4/Au NPs-rGO	0.81	35.59	0.43	63.17

Table S3. Optimisation of reaction conditions for oxidation of indole to isatin catalysed by Fe_3O_4/Au NPs-rGO[a]

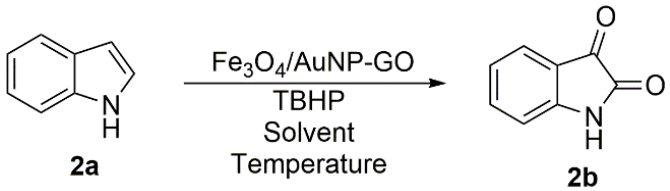

Sl. No.	Catalyst (mg)	TBHP (µL)	Solvent	Temp. (º C)	% Yield[b]
1	0.1	-	Toluene	25	[c]
2	0.1	100	Toluene	25	30
3	0.1	100	MeOH	25	40
4	0.1	100	Isopropanol	25	32
5	0.1	100	Water	25	31
6	0.1	100	EtOH	25	28
7	0.1	100	DCM	25	Traces
8	0.1	100	MeOH	80	56
9	**0.1**	**100**	**ACN**	**25**	**75**
10	0.1	100	ACN	50	74
11	0.1	100	ACN	80	78
12	0.1	100	ACN	100	72
13	0.1	100	ACN	25	65[d]
14	0.1	100	ACN	25	45[e]
15	0.1	100	ACN	25	77[f]
16	0.1	100	ACN	25	78[g]
17	0.1	100	ACN	25	77[h]
18	0.1	100	ACN	25	69[i]
19	0.1	100	ACN	25	64[j]
20	0.1	1	ACN	25	24
21	0.1	5	ACN	25	30
22	0.1	10	ACN	25	33
23	0.001	100	ACN	25	28
24	0.01	100	ACN	25	45

[a]Reaction conditions: **2a** (0.5 mmol), catalyst Fe_3O_4/Au NPs-rGO(0.1 mg) in solvent (3 mL) for 6 h. [b]Isolated yield. [c]No conversion was detected. Reaction for 3h[d], 1h[e], 12[f] and 24h[g]. Reaction with solvent amount of 2mL[h], 1 mL[i] and 10 mL[j].

Table S4. Scope of reaction for oxidation of indole to isatin catalysed by Fe_3O_4/Au NPs-rGO

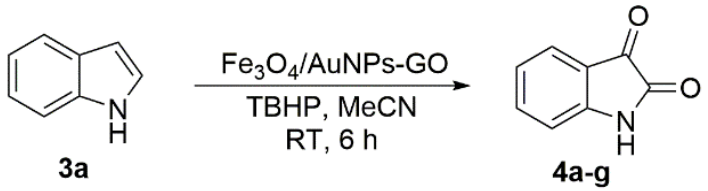

3a 4a-g

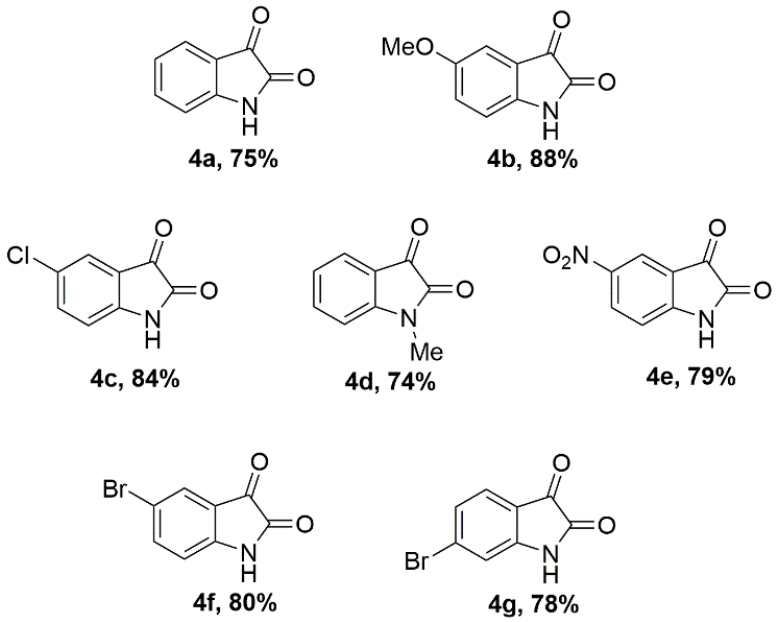

[a]Reaction conditions: **3a** (0.5 mmol), catalyst Fe_3O_4/Au NPs-rGO (0.1 mg) in MeCN (3 mL) for 6 h at RT.

Table S5. Optimisation of reaction conditions for synthesis of spirooxindole catalysed by Fe_3O_4/Au NPs-rGO[a]

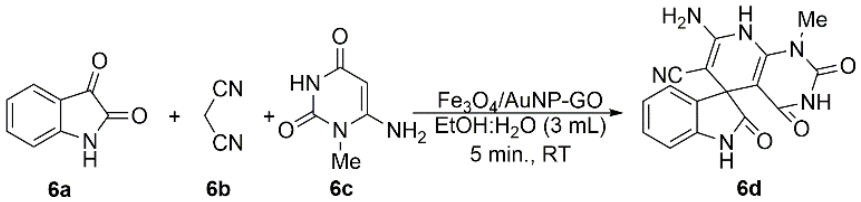

6a 6b 6c 6d

Sl. No.	Catalyst (mg)	Ratio of amount of substrate (5a:5b:5c)	Solvent	% Yield[b]
1	0.1	1:1:1	-	[c]
2	0.1	1:1:1	EtOH	70
3	0.1	1:1:1	MeOH	72
4	0.1	1:1:1	Isopropanol	65
5	0.1	1:1:1	Water	60
6	**0.1**	**1:1:1**	**EtOH;Water (1:1)**	**80**
7	0.1	1:1:1	EtOH;Water (2:1)	75
8	0.1	1:1:1	EtOH;Water (1:2)	70
9	0.1	2:1:1	EtOH;Water (1:1)	76
10	0.1	1:2:1	EtOH;Water (1:1)	79
11	0.1	1:1:2	EtOH;Water (1:1)	77
12	0.001	1:1:1	EtOH;Water (1:1)	40
13	0.01	1:1:1	EtOH;Water (1:1)	37
14	0.1	1:1:1	EtOH;Water (1:1)	79[d]
15	0.1	1:1:1	EtOH;Water (1:1)	56[e]
16	0.1	1:1:1	EtOH;Water (1:1)	80[f]
17	0.1	1:1:1	EtOH;Water (1:1)	68[g]
18	0.1	1:1:1	EtOH;Water (1:1)	55[h]

[a]Reaction conditions: **6a** (0.5 mmol), **6b** (0.5 mmol), **6c** (0.5 mmol), catalyst Fe_3O_4/Au NPs-rGO (0.1 mg) in solvent (3 mL) for 5 min. [b]Isolated yield. [c]No conversion was detected. Reaction at 40 ^oC[d] and 80 ^oC[e] Reaction for 10 min[f], 3 min[g] and 2 min[h].

Table S6. Scope of reaction for the synthesis of spirooxindole catalysed by Fe_3O_4/Au NPs-GO[a]

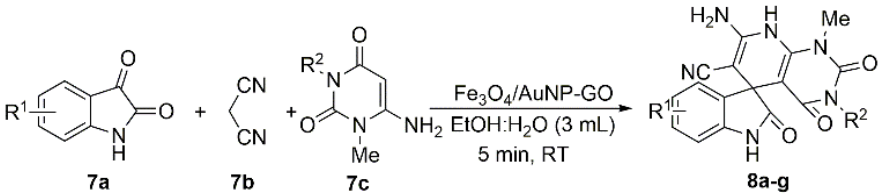

7a 7b 7c 8a-g

8a, 80% 8b, 72% 8c, 93%

8d, 78% 8e, 85%

8f, 80% 8g, 90% 8h, 81%

8i, 95% 8j, 88%

[a]Reaction conditions: **7a** (0.5 mmol), **7b** (0.5 mmol), **7c** (0.5 mmol), catalyst Fe_3O_4/Au NPs-rGO (0.1 mg) in solvent (3 mL) for 5 min.

(8) Physical and Spectroscopic Data of Compounds

Indoline-2,3-dione (Table 3, entry 3a)

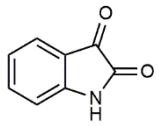

Orange solid; 75%; m.p. 198 ˚C;^{1}H NMR (400 MHz, DMSO-d_6): δ= 11.66 (s, 1H), 8.44 (dd, J = 8.8, 2.6 Hz, 1H), 8.21 (d, J = 2.8 Hz, 1H), 7.09 (d, J = 8.8 Hz, 1H) ppm; ^{13}C NMR (100 MHz, DMSO-d_6): δ= 184.4, 159.4, 150.7, 138.4, 124.7, 122.8, 117.9, 112.2 ppm; IR (KBr) $\tilde{\nu}$= 3451, 1737, 1620, 1466, 1327 cm^{-1}.

5-Methoxyindoline-2,3-dione (Table 3, entry 3b)

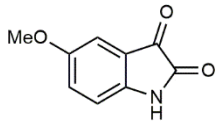

Red solid; 88%; m.p. 199 ˚C; ^{1}H NMR (400 MHz, DMSO-d_6): δ= δ 10.84 (s, 1H), 7.18 (dd, J = 8.6, 2.9 Hz, 1H), 7.07 (d, J = 3.3 Hz, 1H), 6.84 (d, J = 8.6 Hz, 1H), 3.74 (s, 3H) ppm; ^{13}C NMR (100MHz, DMSO-d_6): δ= 184.7, 159.6, 155.3, 144.7, 124.9, 118.1, 113.2, 108.8, 55.8 ppm; IR (KBr) $\tilde{\nu}$= 3441, 3182, 1644, 1749, 1308 cm^{-1}.

5-Chloroindoline-2,3-dione (Table 3, entry 3c)

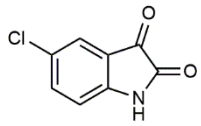

Orange solid; 84%; m.p. >200 ˚C; ^{1}H NMR (400 MHz, DMSO-d_6): δ= 11.13 (s, 1H), 7.99-7.43 (m, 2H), 6.92 (d, J = 8.6 Hz, 1H) ppm; ^{13}C NMR (100 MHz, DMSO-d_6): δ= 183.4, 159.2, 149.2, 137.3, 126.8, 124.2, 119.2, 113.9 ppm; IR (KBr) $\tilde{\nu}$= 3462, 3185, 1755, 1709, 1611 cm^{-1}.

5-Nitroindoline-2,3-dione (Table 3, entry 3d)

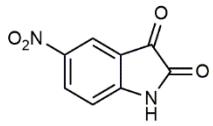

Yellow solid; 79%; m.p. >200 ˚C; ^{1}H NMR (400 MHz, DMSO-d_6): δ= 11.66 (s, 1H), 8.44 (dd, J = 8.8, 2.5 Hz, 1H), 8.21 (d, J = 2.7 Hz, 1H), 7.08 (d, J = 9.2 Hz, 1H) ppm; ^{13}C NMR (100 MHz, DMSO-d_6): δ= 182.4, 159.9, 155.2, 142.6, 133.1, 119.6, 118.1, 112.5 ppm; IR (KBr) $\tilde{\nu}$= 3335, 1764, 1615, 1536, 1326 cm^{-1}.

1-Methylindoline-2,3-dione (Table 3, entry 3e)

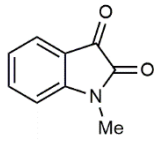

Brown solid; 74%; m.p. 131 ˚C; ^{1}H NMR (400 MHz, DMSO-d_6): δ= 11.03 (s, 1H), 7.53 (m, 1H), 7.06 (td, J = 7.6, 1.0 Hz, 1H), 6.94-6.87 (m, 1H), 3.33 (s, 3H) ppm; ^{13}C NMR (100 MHz, DMSO-d_6): δ= 183.53, 158.19, 151.38, 138.17, 124.28, 123.19, 117.40, 110.65 ppm; IR (KBr) $\tilde{\nu}$= 3448, 2926, 1733, 1613, 1465 cm^{-1}.

5-Bromoindoline-2,3-dione (Table 3, entry 3f)

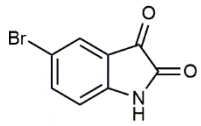

Brown solid; 80%; m.p. >200 ˚C; ^{1}H NMR (400 MHz, Methanol-d_4): δ= 7.59 (dd, J = 2.0, 0.6 Hz, 1H), 7.25 (dd, J = 8.6, 0.6 Hz, 1H), 7.15 (dd, J = 8.8, 2.2 Hz, 1H), 7.01 (s, 1H) ppm; ^{13}C NMR (100 MHz, DMSO-d_6): δ= 183.9, 159.7, 149.7, 137.8, 127.3, 124.6, 119.7, 114.3 ppm; IR (KBr) $\tilde{\nu}$= 3444, 2923, 1762, 1248, 1049 cm^{-1}.

6-Bromoindoline-2,3-dione (Table 3, entry 3g)

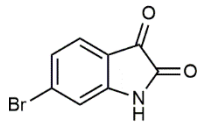

Brown solid; 78%; m.p. >200 ˚C; ^{1}H NMR (400 MHz, Methanol-d_4): δ= 7.50 (dd, J = 1.9, 0.6 Hz, 1H), 7.39 (dd, J = 8.5, 0.6 Hz, 1H), 7.06 (dd, J = 8.5, 1.8 Hz, 1H), 6.99 (t, J = 1.1 Hz, 1H) ppm; ^{13}C NMR (100 MHz, DMSO-d_6): δ= 183.8, 159.6, 149.7, 137.8, 127.3, 124.6, 119.6, 114.3 ppm; IR (KBr) $\tilde{\nu}$= 3465, 2992, 1745, 1378, 1242 cm^{-1}.

7'-Amino-1'-methyl-2,2',4'-trioxo-2',3',4',8'-tetrahydro-1'*H*-spiro[indoline-3,5'-pyrido[2,3-*d*]pyrimidine]-6'-carbonitrile (Table 5, entry 6a)

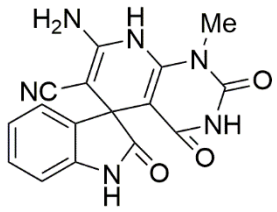

Brick red solid; 80%; m.p. >200 ˚C;^{1}H NMR (400 MHz, DMSO-d_6): δ= 11.21 (s, 1H), 10.31 (s, 1H), 7.89 (d, J = 8.5 Hz, 1H), 7.57 (t, J = 8.4 Hz, 1H), 7.14 (t, J = 8.3 Hz, 1H), 6.94 (d, J = 8.3 Hz, 1H), 6.76 (s, 1H), 4.54 (d, J = 2.4 Hz, 1H), 3.17 (s, 3H), 2.08 (s, 1H) ppm; ^{13}C NMR (100 MHz, DMSO-d_6): δ= 163.8, 162.3, 156.4, 151.3, 150.7, 146.5, 137.8, 125.9, 122.9, 118.7, 113.1, 111.7, 111.6, 80.6, 75.2 ppm; IR (KBr) $\tilde{\nu}$= 3429, 3261, 1716, 1616, cm^{-1}.

7'-Amino-1',3'-dimethyl-2,2',4'-trioxo-2',3',4',8'-tetrahydro-1'*H*-spiro[indoline-3,5'-pyrido[2,3-*d*]pyrimidine]-6'-carbonitrile(Table 5, entry 6b)

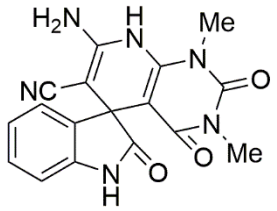

Red solid; 72%; m.p. >200 ˚C; ^{1}H NMR (400 MHz, DMSO-d_6): δ= 11.21 (s, 1H), 7.88 (d, J = 8.5 Hz, 1H), 7.57 (td, J = 7.9, 1.3 Hz, 1H), 7.14 (td, J = 7.8, 1.1 Hz, 1H), 6.94 (d, J = 8.0 Hz, 1H), 3.23 (s, 1H), 3.06 (s, 1H) ppm; ^{13}C NMR (100 MHz, DMSO-d_6): δ= 163.9, 150.8, 146.5, 137.9, 137.9, 125.9, 123.0, 122.9, 118.7, 113.1, 111.7, 111.7, 111.6, 80.7 ppm; IR (KBr) $\tilde{\nu}$= 3439, 3261, 1715, 1627, 1586 cm^{-1}.

7'-Amino-5-methoxy-1'-methyl-2,2',4'-trioxo-2',3',4',8'-tetrahydro-1'*H*-spiro[indoline-3,5'-pyrido[2,3-*d*]pyrimidine]-6'-carbonitrile (Table 5, entry 6c)

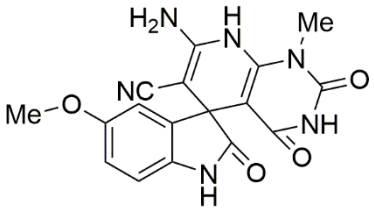

Black solid; 93%; m.p. >200 ˚C; ^{1}H NMR (400 MHz, DMSO-d_6): δ= 11.01 (s, 1H), 7.38 (d, J = 2.9 Hz, 1H), 7.21 (dd, J = 8.7, 2.7 Hz, 1H), 6.87 (d, J = 8.7 Hz, 1H), 6.76 (s, 1H), 4.54 (d, J = 2.4 Hz, 1H), 3.75 (s, 5H), 3.16 (s, 3H) ppm; ^{13}C NMR (100 MHz, DMSO-d_6): δ= 163.8, 162.4, 156.4, 151.3, 150.9, 140.6, 124.2, 119.1, 113.09, 112.6, 111.5, 110.2, 80.91 75.2, 55.8 ppm; IR (KBr) $\tilde{\nu}$= 3385, 3177, 1713, 1588, 1491 cm^{-1}.

7'-Amino-5-methoxy-1',3'-dimethyl-2,2',4'-trioxo-2',3',4',8'-tetrahydro-1'*H*-spiro[indoline-3,5'-pyrido[2,3-*d*]pyrimidine]-6'-carbonitrile(Table 5, entry 6d)

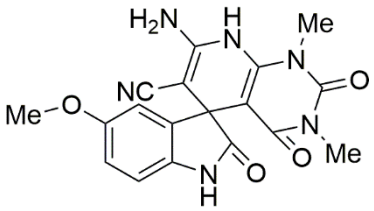

Royal Blue solid; 78%; m.p. >200 ˚C; ^{1}H NMR (400 MHz, DMSO-d_6): δ= 11.00 (s, 1H), 8.31 (s, 1H), 7.38 (d, J = 2.8 Hz, 1H), 7.21 (m, 1H), 6.87 (d, J = 9.0 Hz, 1H), 3.75 (s, 3H) ppm; ^{13}C NMR (100 MHz, DMSO-d_6): δ= 163.8, 154.9, 150.8, 140.6, 124.2, 124.1, 119.1, 113.0, 112.6, 112.5, 111.5, 110.3, 110.2, 80.9, 55.8, 55.7 ppm; IR (KBr) $\tilde{\nu}$= 3388, 2224, 1715, 1592, 1484 cm^{-1}.

7'-Amino-5-chloro-1'-methyl-2,2',4'-trioxo-2',3',4',8'-tetrahydro-1'*H*-spiro[indoline-3,5'-pyrido[2,3-*d*]pyrimidine]-6'-carbonitrile (Table 5, entry 6e)

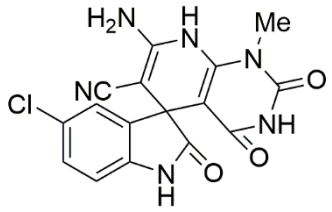

Brown solid; 85%; m.p. >200 ˚C; ^{1}H NMR (400 MHz, DMSO-d_6): δ= 7.91 (d, J = 8.7 Hz, 1H), 7.66 (t, J = 8.6 Hz, 1H), 7.27-7.08 (m, 2H), 3.15 (s, 3H) ppm; ^{13}C NMR (100 MHz, DMSO-d_6): δ= 163.6, 162.4, 156.4, 151.3, 149.7, 145.2, 137.0, 126.5, 124.8, 120.1, 113.4, 112.8, 111.2, 82.4, 75.2, 28.3 ppm; IR (KBr) $\tilde{\nu}$= 3588, 3515, 2983, 1736, 1598 cm^{-1}.

7'-Amino-5-chloro-1',3'-dimethyl-2,2',4'-trioxo-2',3',4',8'-tetrahydro-1'*H*-spiro[indoline-3,5'-pyrido[2,3-*d*]pyrimidine]-6'-carbonitrile (Table 5, entry 6f)

Dark brown solid; 80%; m.p. >200 ˚C; ^{1}H NMR (400 MHz, DMSO-d_6): δ= 11.37 (s, 1H), 7.77 (s, 1H), 7.64 (d, J = 10.7 Hz, 1H), 6.97 (d, J = 8.9 Hz, 1H) ppm; ^{13}C NMR (100 MHz, DMSO-d_6): δ= 163.6, 149.7, 145.2, 137.0, 136.9, 126.5, 124.8, 124.7, 120.0, 113.4, 112.8, 111.2, 82.3 ppm; IR (KBr) $\tilde{\nu}$= 3581, 3513, 2990, 1733, 1596 cm^{-1}.

7'-Amino-1,1'-dimethyl-2,2',4'-trioxo-2',3',4',8'-tetrahydro-1'*H*-spiro[indoline-3,5'-pyrido[2,3-*d*]pyrimidine]-6'-carbonitrile(Table 5, entry 6g)

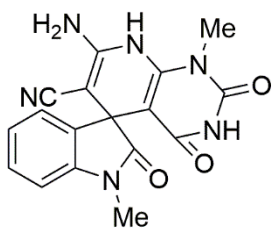

Black solid; 90%; m.p.>200 ˚C; ^{1}H NMR (400 MHz, DMSO-d_6): δ= 11.36 (s, 1H), 7.77 (d, J = 2.3 Hz, 1H), 7.68-7.59 (m, 1H), 6.97 (dd, J = 8.6, 1.6 Hz, 1H) ppm; ^{13}C NMR (100 MHz, DMSO-d_6): δ= 163.5, 149.7, 145.2, 136.9, 136.9, 126.5, 124.8, 124.8, 120.0, 113.4, 113.3, 112.8, 111.2, 82.3 ppm; IR (KBr) $\tilde{\nu}$= 3371, 3180, 2235, 1722, 1598 cm^{-1}.

7'-Amino-1,1',3'-trimethyl-2,2',4'-trioxo-2',3',4',8'-tetrahydro-1'*H*-spiro[indoline-3,5'-pyrido[2,3-*d*]pyrimidine]-6'-carbonitrile (Table 5, entry 6h)

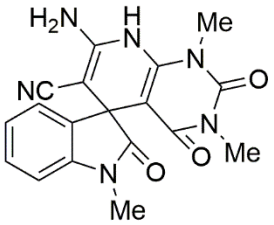

Dark brown solid; 81%; m.p. >200 ˚C; ^{1}H NMR (400 MHz, DMSO-d_6): δ= 7.91 (d, J = 5.7 Hz, 2H), 7.67 (dd, J = 9.1, 6.1 Hz, 2H), 7.16 (tt, J = 15.2, 7.6 Hz, 5H), 3.15 (s, 6H), 3.13 (s, 1H) ppm; ^{13}C NMR (100 MHz, DMSO-d_6): δ= 183.5, 162.5, 158.2, 151.4, 149.8, 147.2, 137.7, 137.7, 125.5, 118.1, 117.4, 112.9, 111.5, 110.6, 110.5, 81.2, 26.3, 26.3 ppm; IR (KBr) $\tilde{\nu}$= 3427, 2231, 1718, 1594, 1469 cm^{-1}.

7'-Amino-1'-methyl-5-nitro-2,2',4'-trioxo-2',3',4',8'-tetrahydro-1'*H*-spiro[indoline-3,5'-pyrido[2,3-*d*]pyrimidine]-6'-carbonitrile (Table 5, entry 6i)

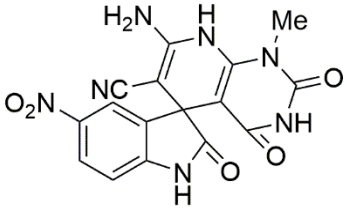

Red solid; 95%; m.p. >200 ˚C; ^{1}H NMR (400 MHz, DMSO-d_6): δ= 11.93 (s, 1H), 10.31 (s, 1H), 8.66 (s, 1H), 8.45 (d, J = 10.9 Hz, 1H), 7.15 (d, J = 9.0 Hz, 1H), 6.77 (s, 1H), 3.16 (s, 3H) ppm; ^{13}C NMR (100 MHz, DMSO-D6): δ= 179.9, 160.4, 150.9, 149.9, 148.3, 146.5, 142.4, 137.4, 125.6, 119.2, 118.3,109.19, 85.6, 56.9, 49.2, 29.1 ppm; IR (KBr) $\tilde{\nu}$= 3580, 3522, 2829, 1729, 1338 cm^{-1}.

7'-Amino-1',3'-dimethyl-5-nitro-2,2',4'-trioxo-2',3',4',8'-tetrahydro-1'*H*-spiro[indoline-3,5'-pyrido[2,3-*d*]pyrimidine]-6'-carbonitrile (Table 5, entry 6j)

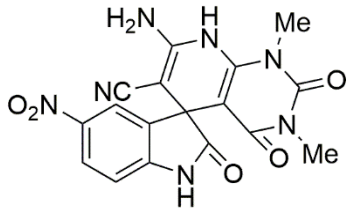

Red solid; 88%; m.p. >200 ˚C; ^{1}H NMR (400 MHz, DMSO-d_6): δ= 11.94 (s, 1H), 8.65 (s, 1H), 8.45 (d, J = 10.7 Hz, 1H), 7.14 (d, J = 10.2 Hz, 1H) ppm; ^{13}C NMR (100 MHz, DMSO-d_6): δ= 164.1, 151.2, 149.3, 142.4, 132.7, 120.7, 118.8, 112.6, 111.9, 110.9, 83.5 ppm; IR (KBr) $\tilde{\nu}$= 3583, 3512, 2839, 1728, 1341 cm^{-1}.

(9) ^{1}H NMR and ^{13}C NMR spectra of compounds

Indoline-2,3-dione (Table 3, entry 3a)

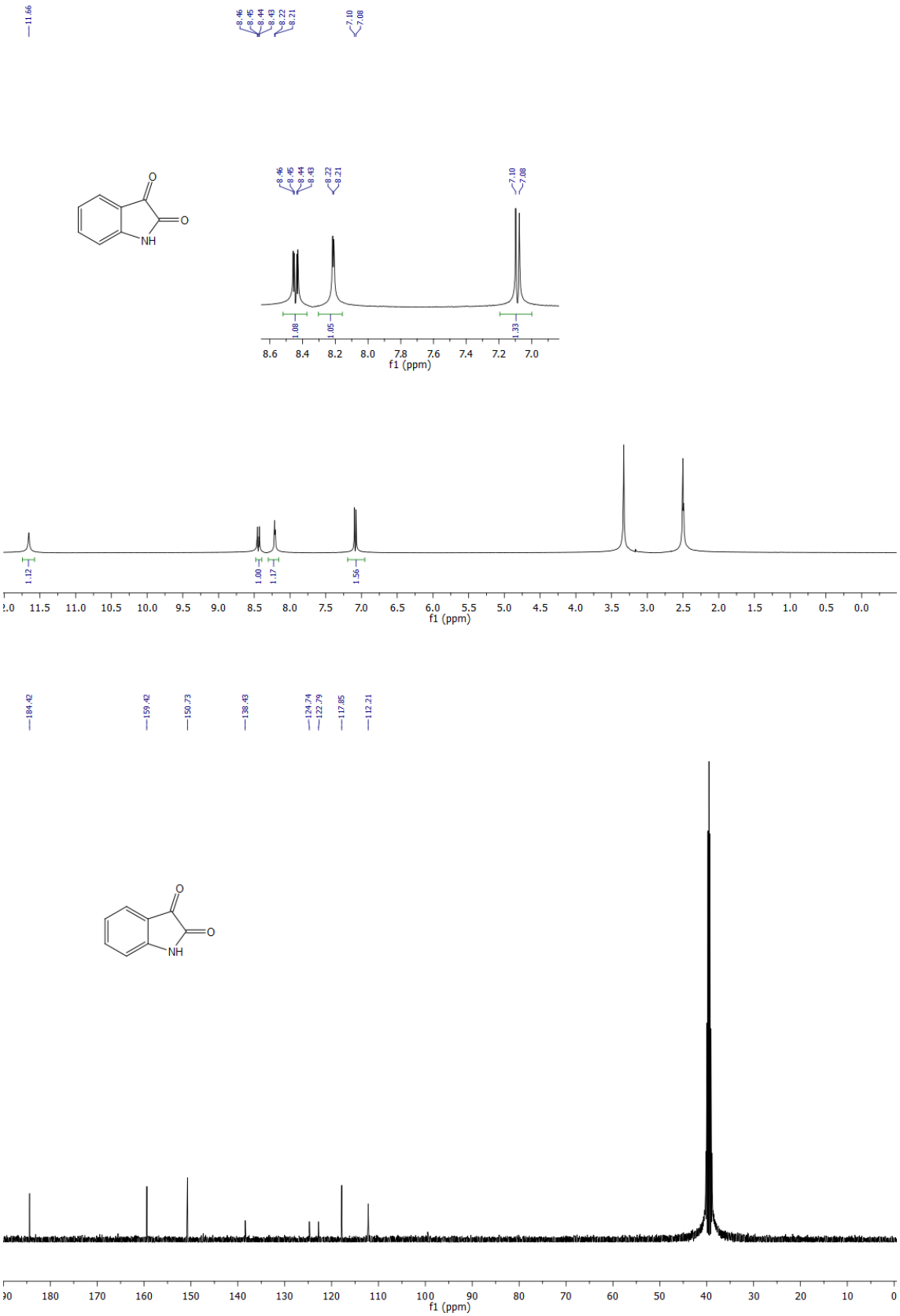

5-Methoxyindoline-2,3-dione (Table 3, entry 3b)

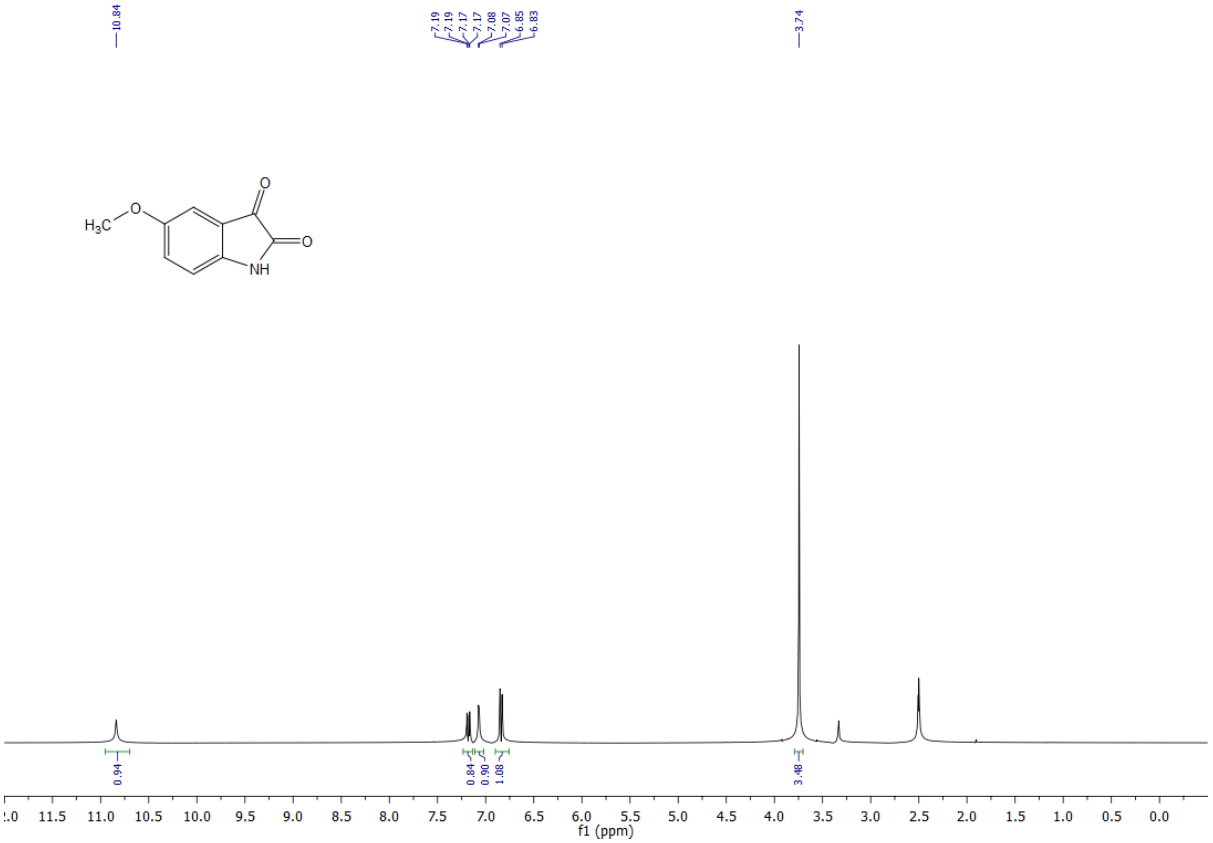

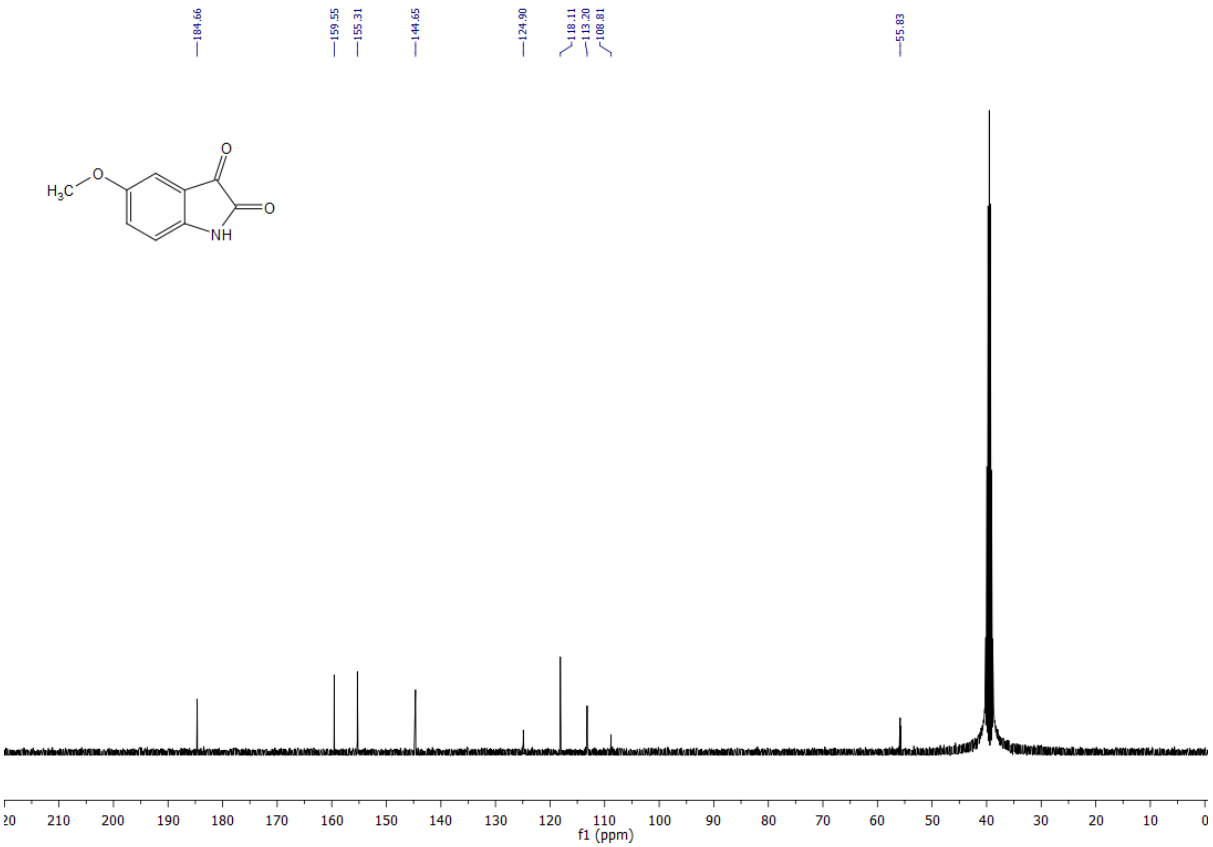

5-Chloroindoline-2,3-dione (Table 3, entry 3c)

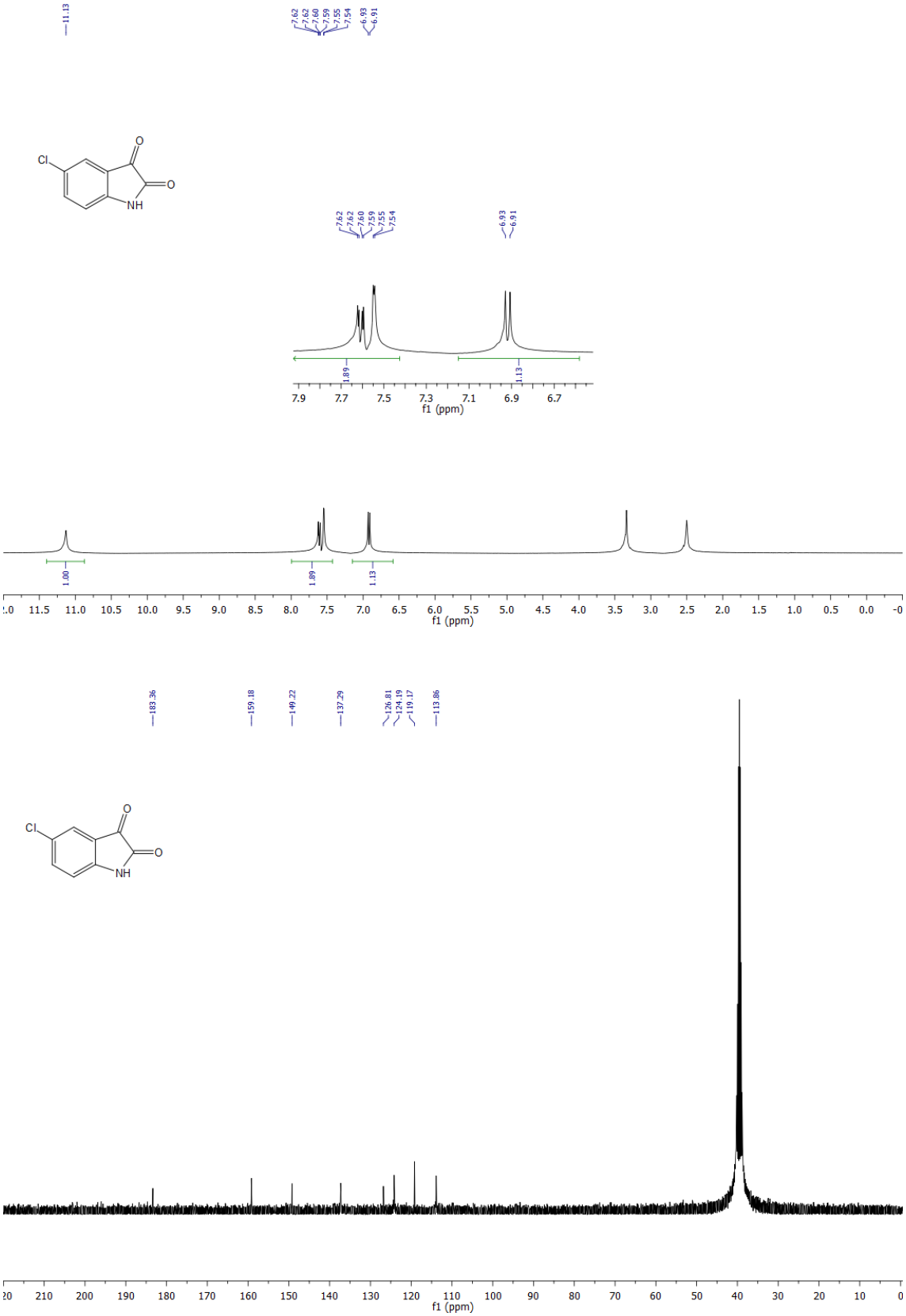

5-Nitroindoline-2,3-dione (Table 3, entry 3d)

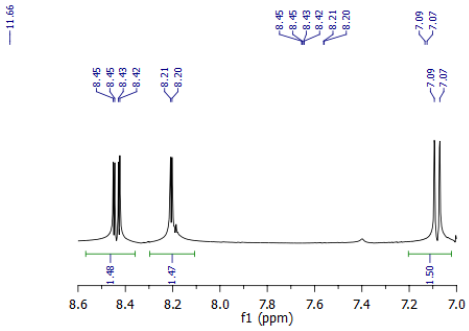

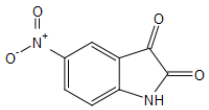

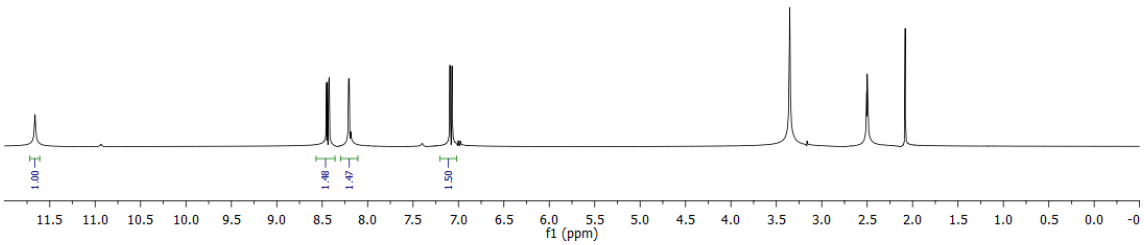

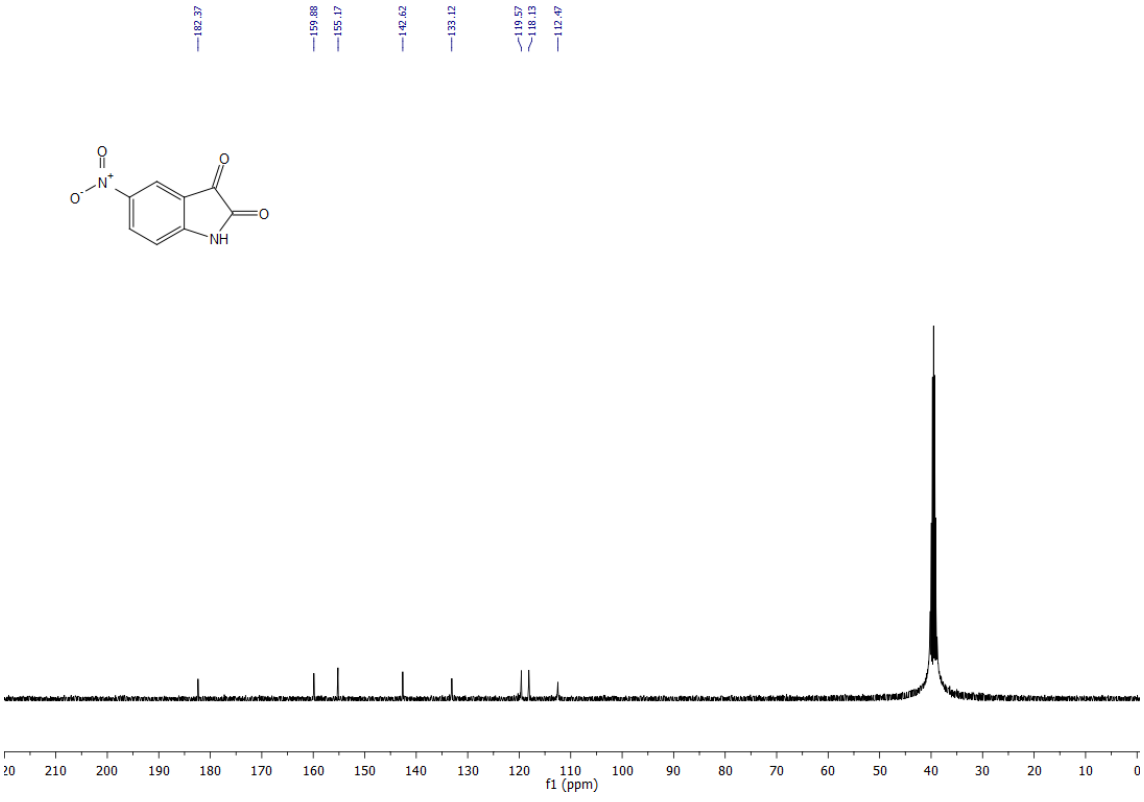

1-Methylindoline-2,3-dione (Table 3, entry 3e)

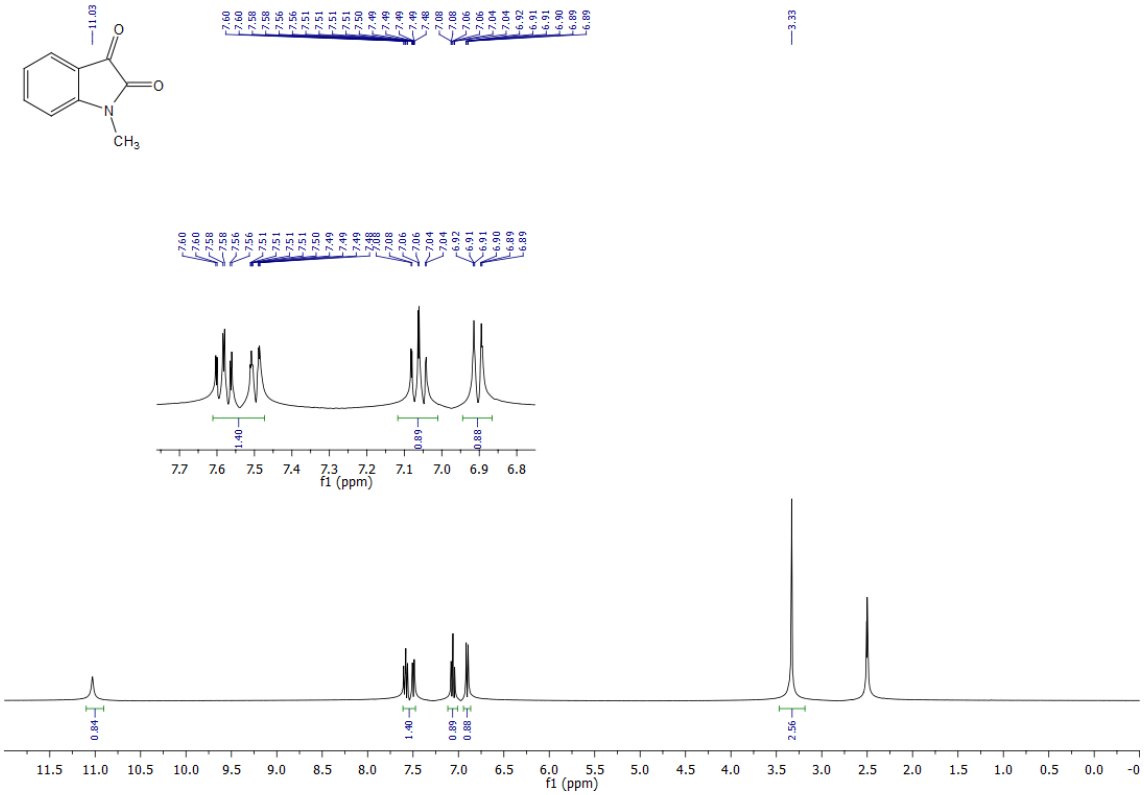

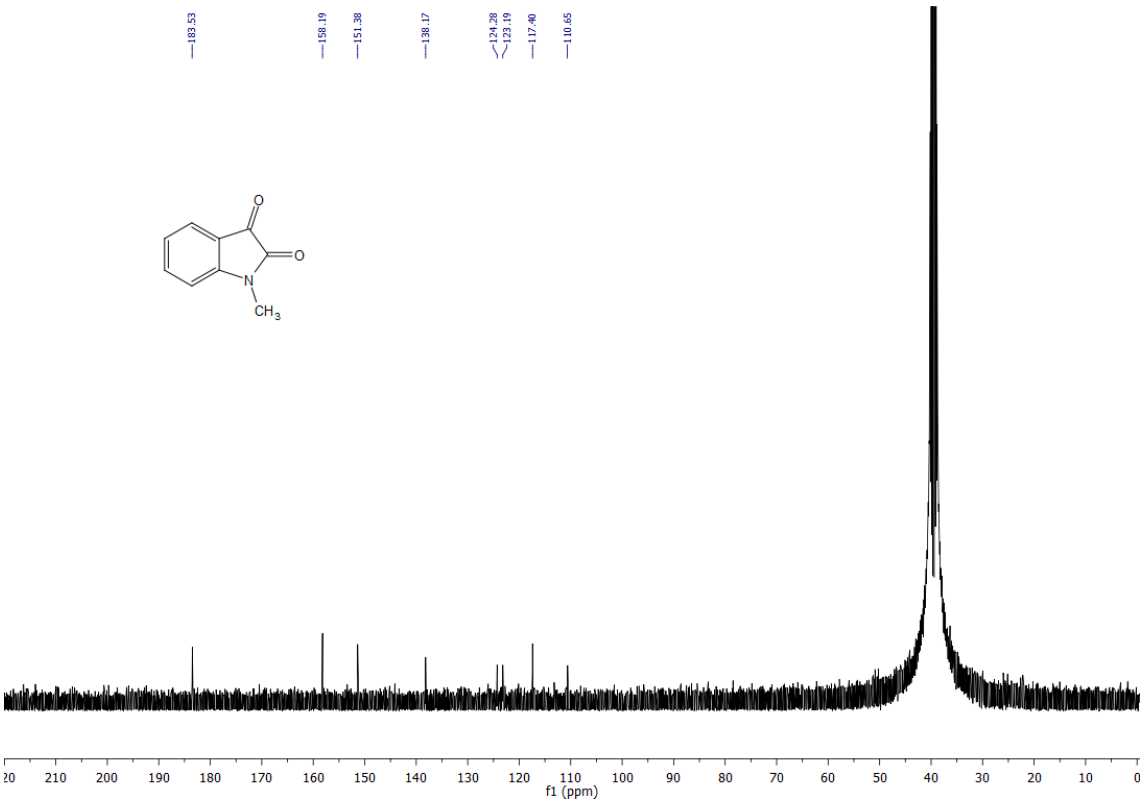

5-Bromoindoline-2,3-dione (Table 3, entry 3f)

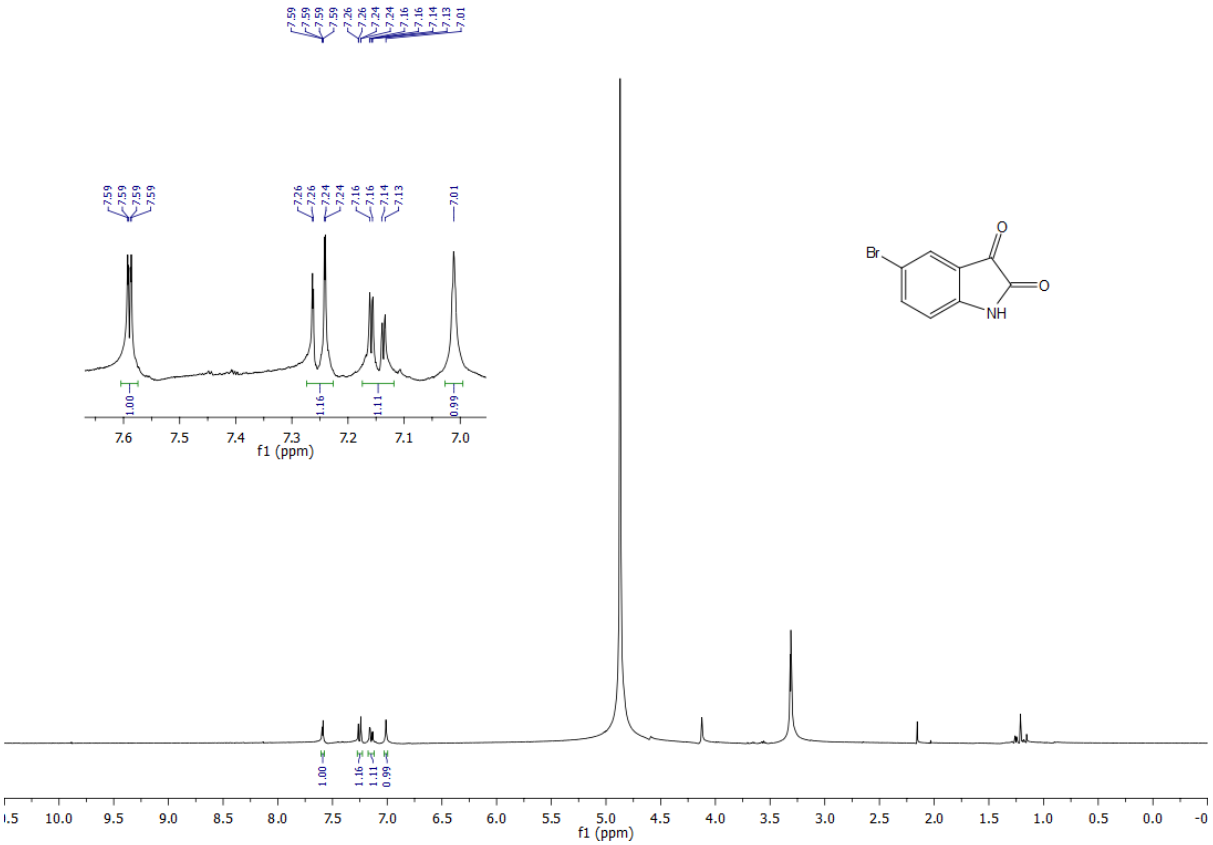

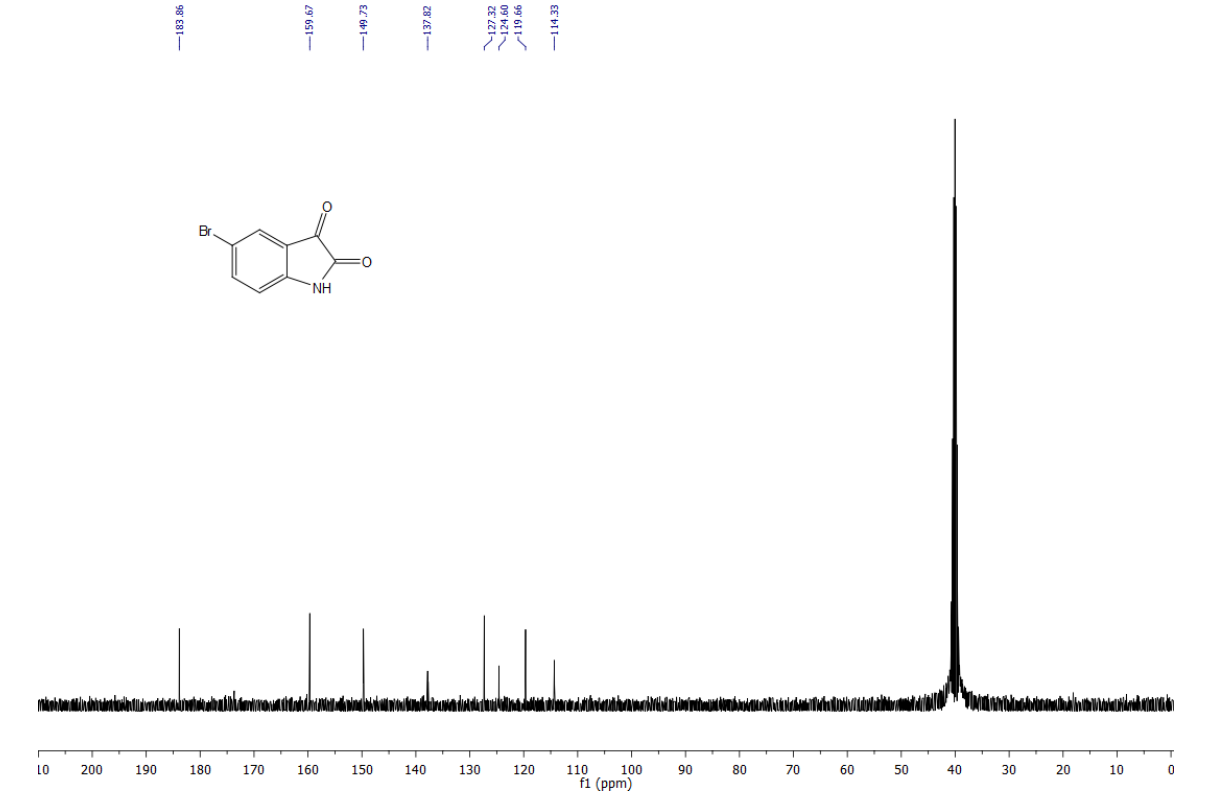

6-Bromoindoline-2,3-dione (Table 3, entry 3g)

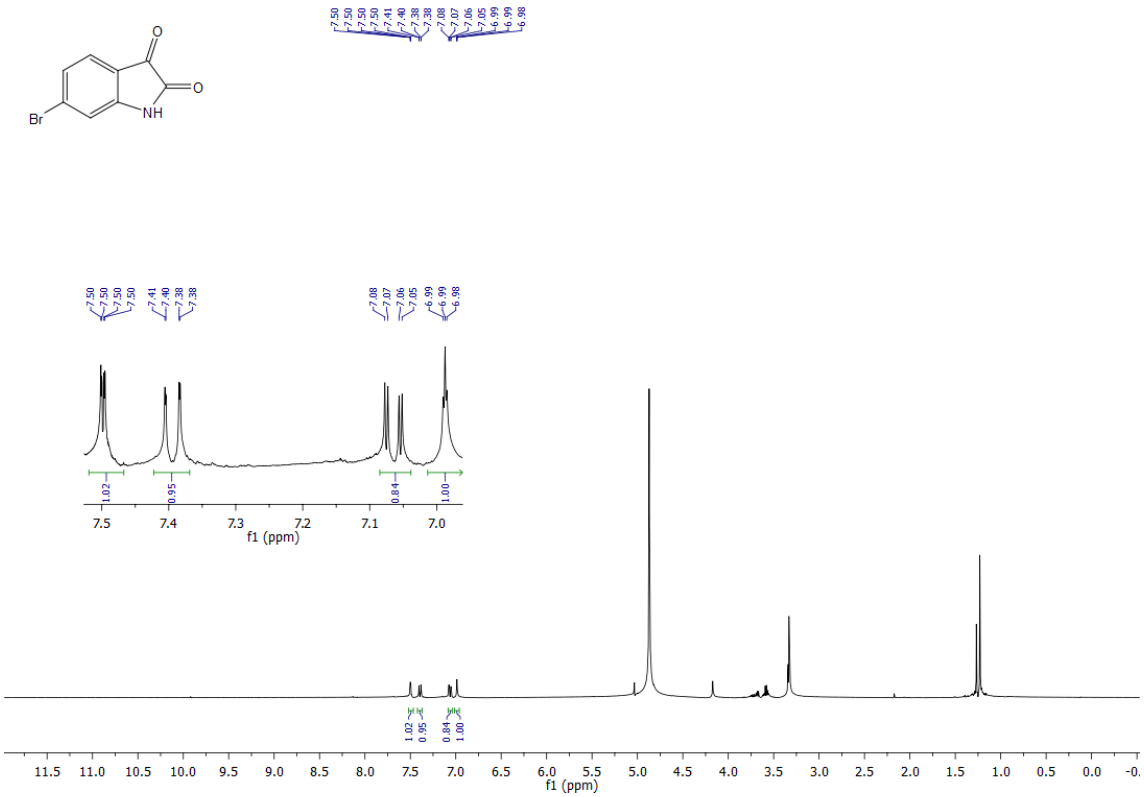

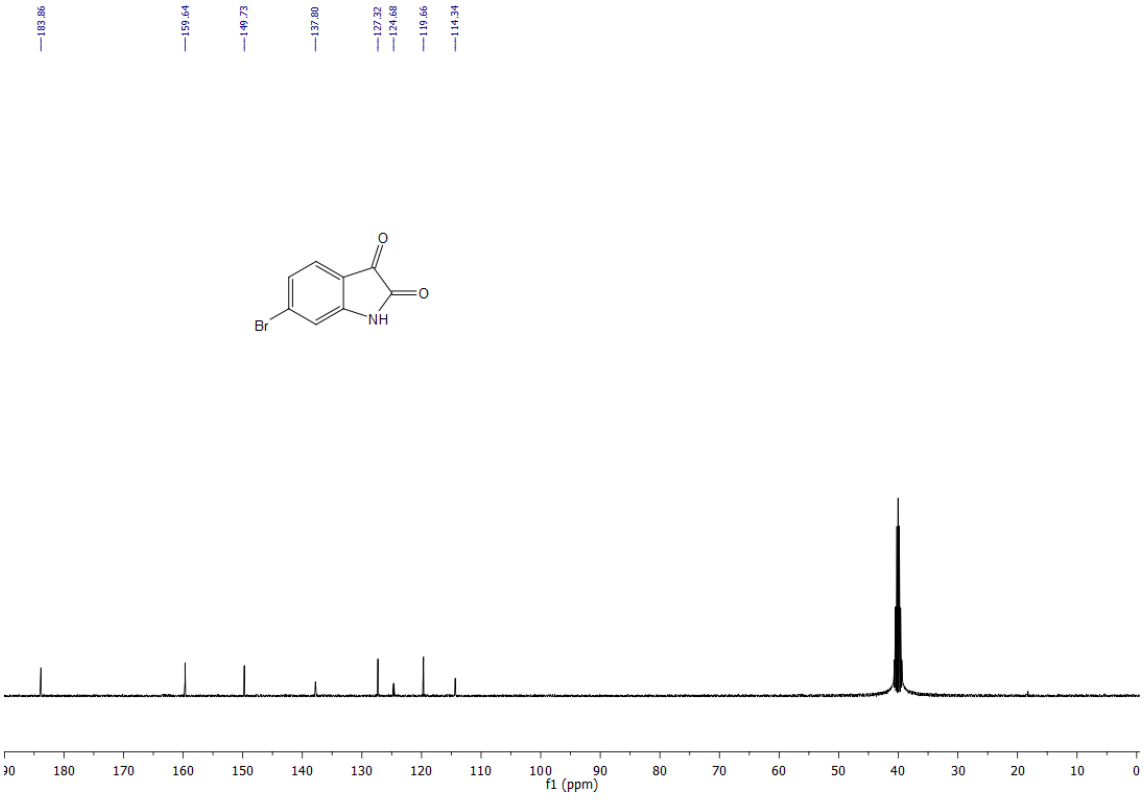

7'-Amino-1'-methyl-2,2',4'-trioxo-2',3',4',8'-tetrahydro-*1'H*-spiro[indoline-3,5'-pyrido[2,3-*d*]pyrimidine]-6'-carbonitrile (Table 5, entry 6a)

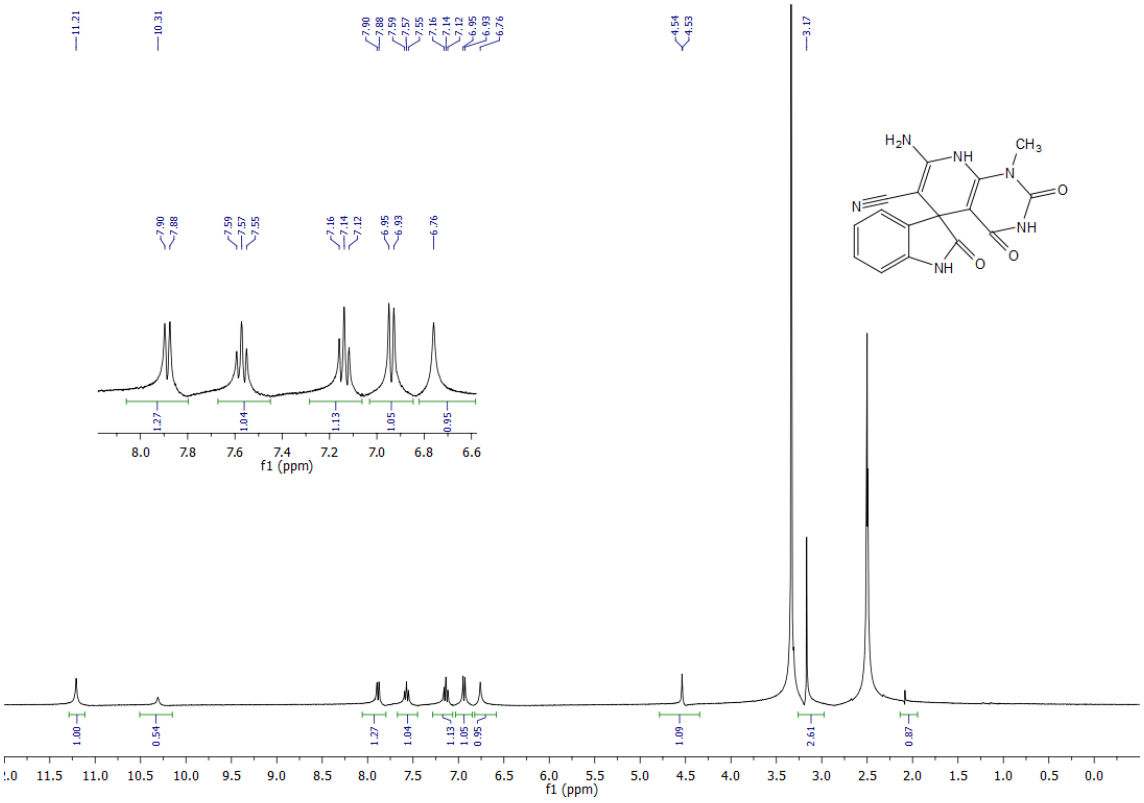

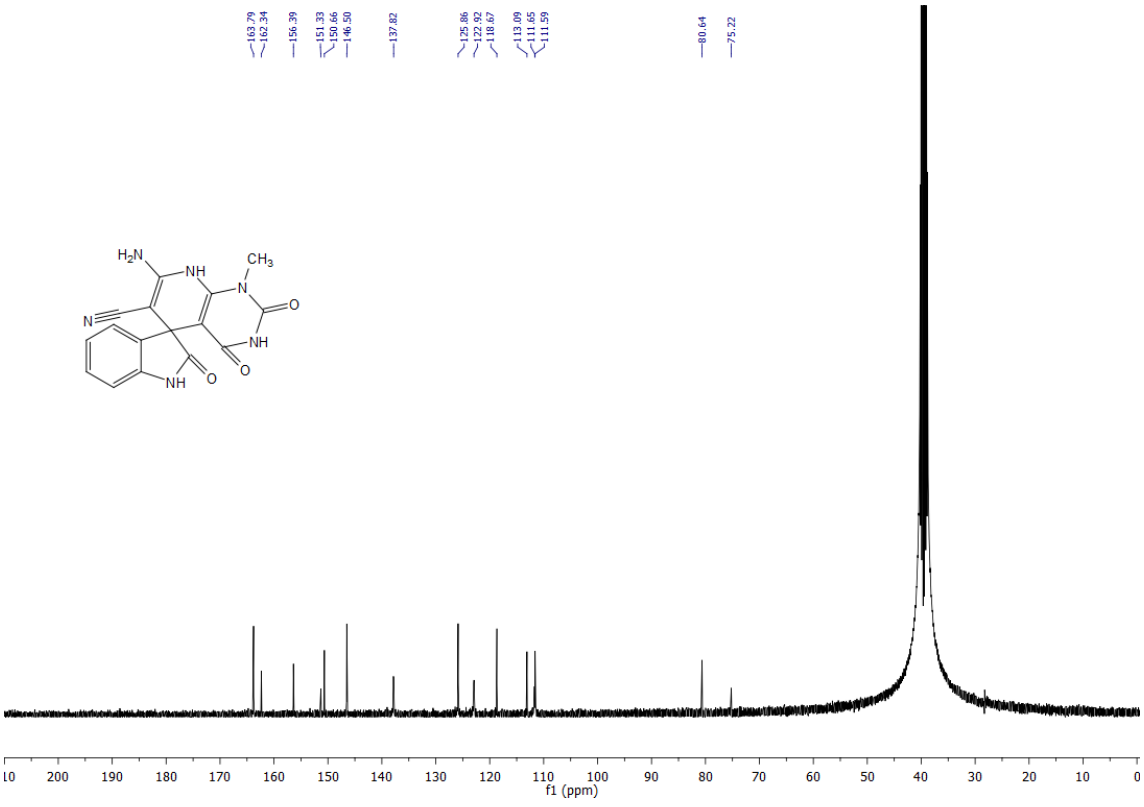

7'-Amino-1',3'-dimethyl-2,2',4'-trioxo-2',3',4',8'-tetrahydro-1'*H*-spiro[indoline-3,5'-pyrido[2,3-*d*]pyrimidine]-6'-carbonitrile (Table 5, entry 6b)

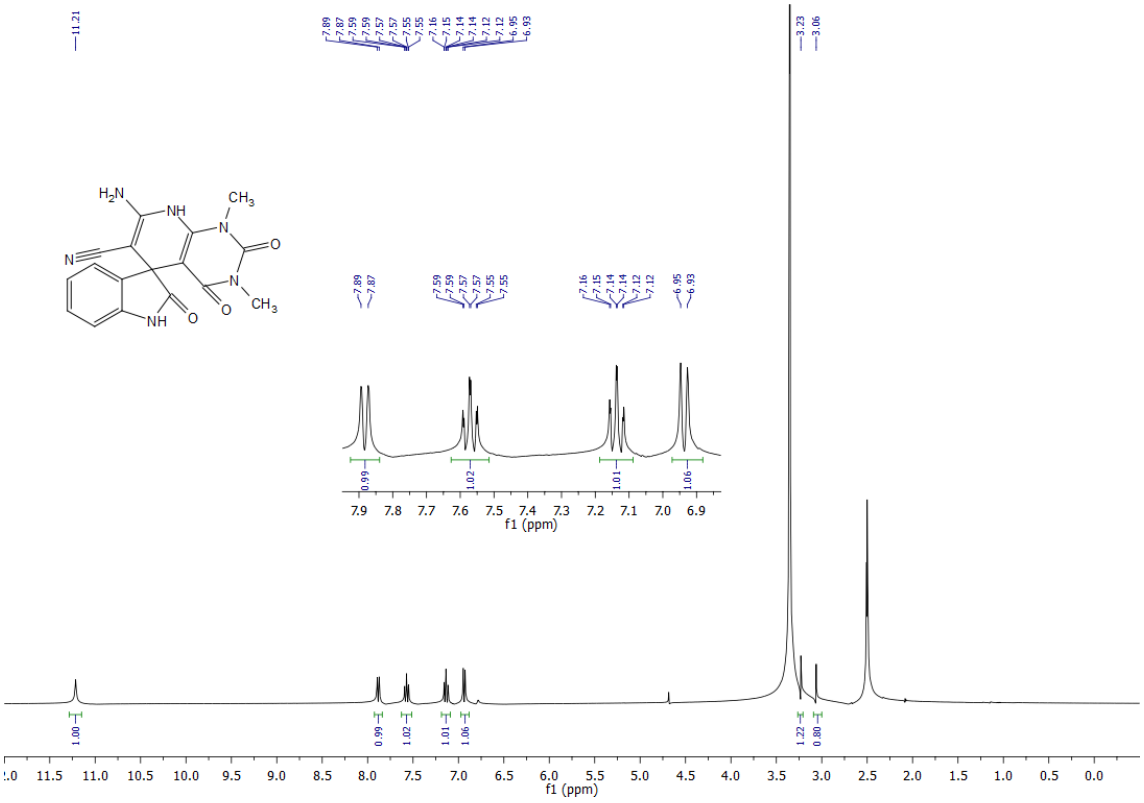

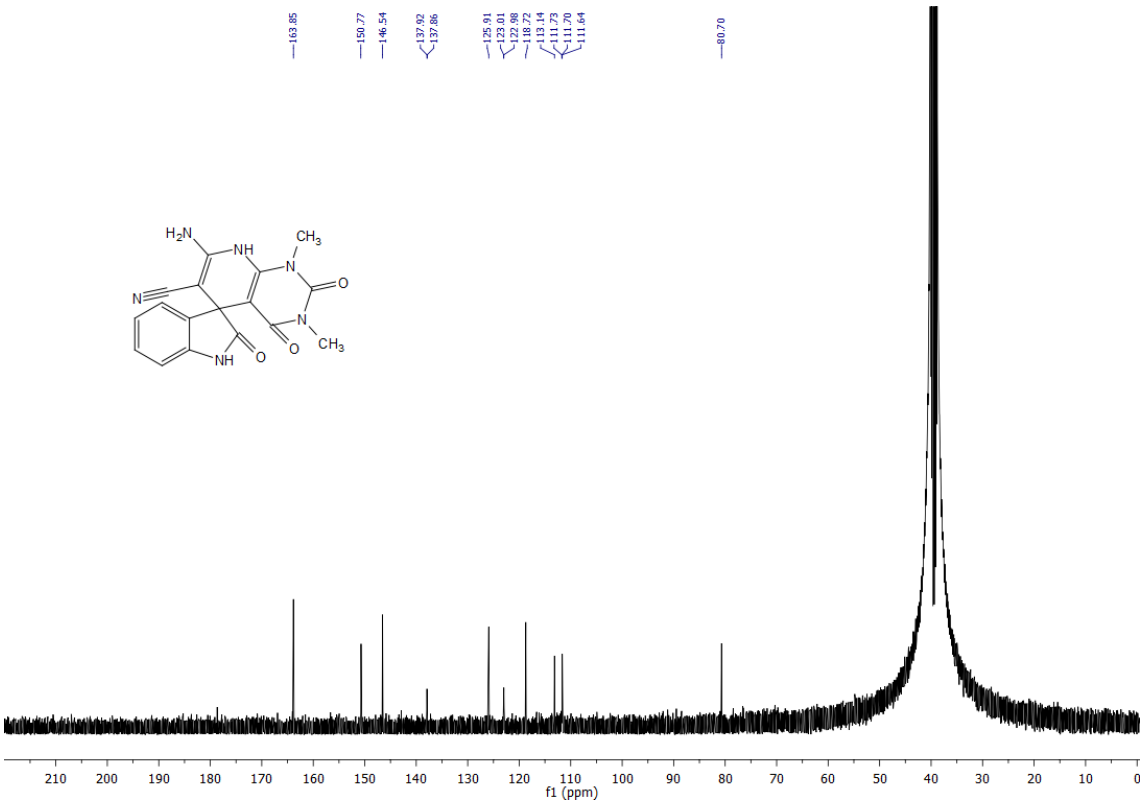

7'-Amino-5-methoxy-1'-methyl-2,2',4'-trioxo-2',3',4',8'-tetrahydro-1'*H*-spiro[indoline-3,5'-pyrido[2,3-*d*]pyrimidine]-6'-carbonitrile (Table 5, entry 6c)

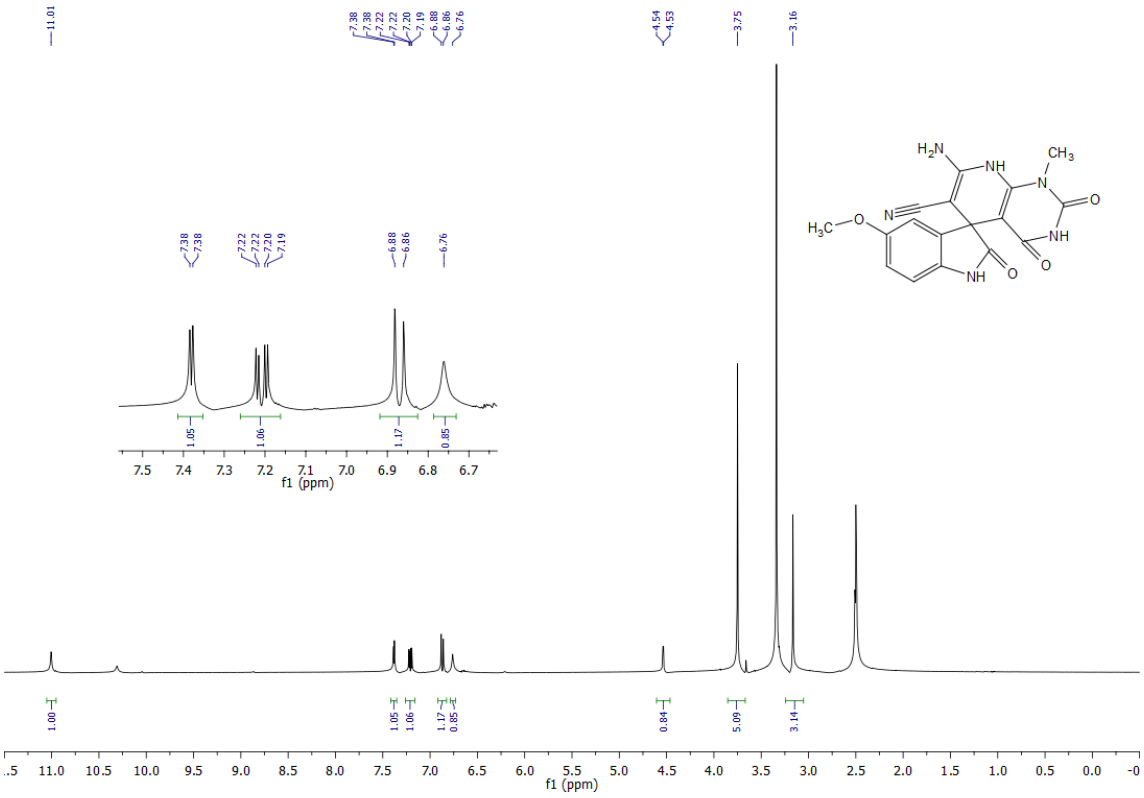

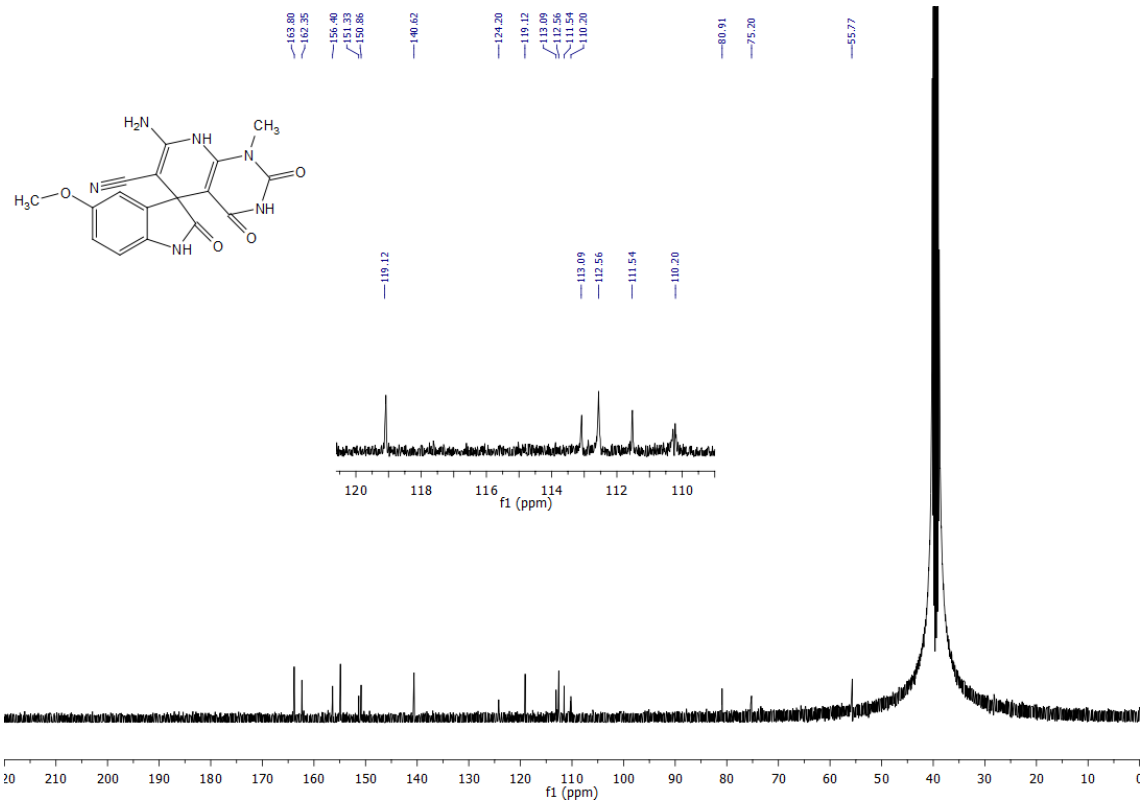

7'-Amino-5-methoxy-1',3'-dimethyl-2,2',4'-trioxo-2',3',4',8'-tetrahydro-1'*H*-spiro[indoline-3,5'-pyrido[2,3-*d*]pyrimidine]-6'-carbonitrile (Table 5, entry 6d)

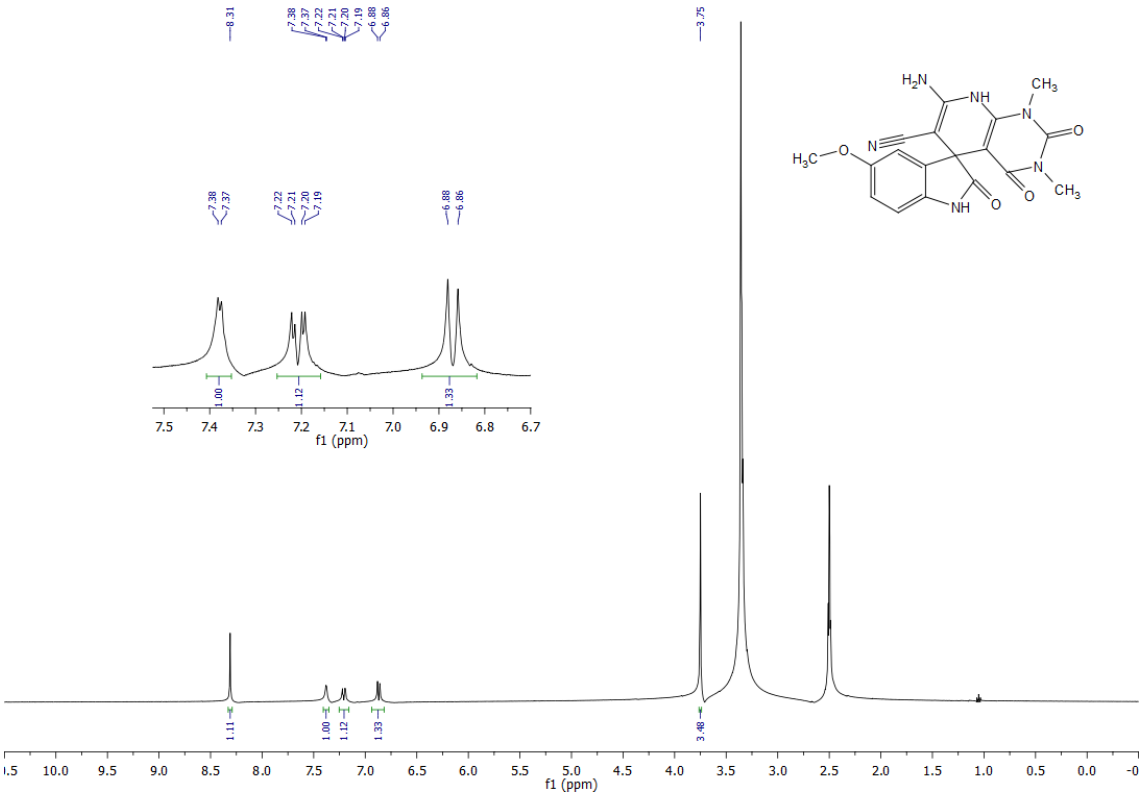

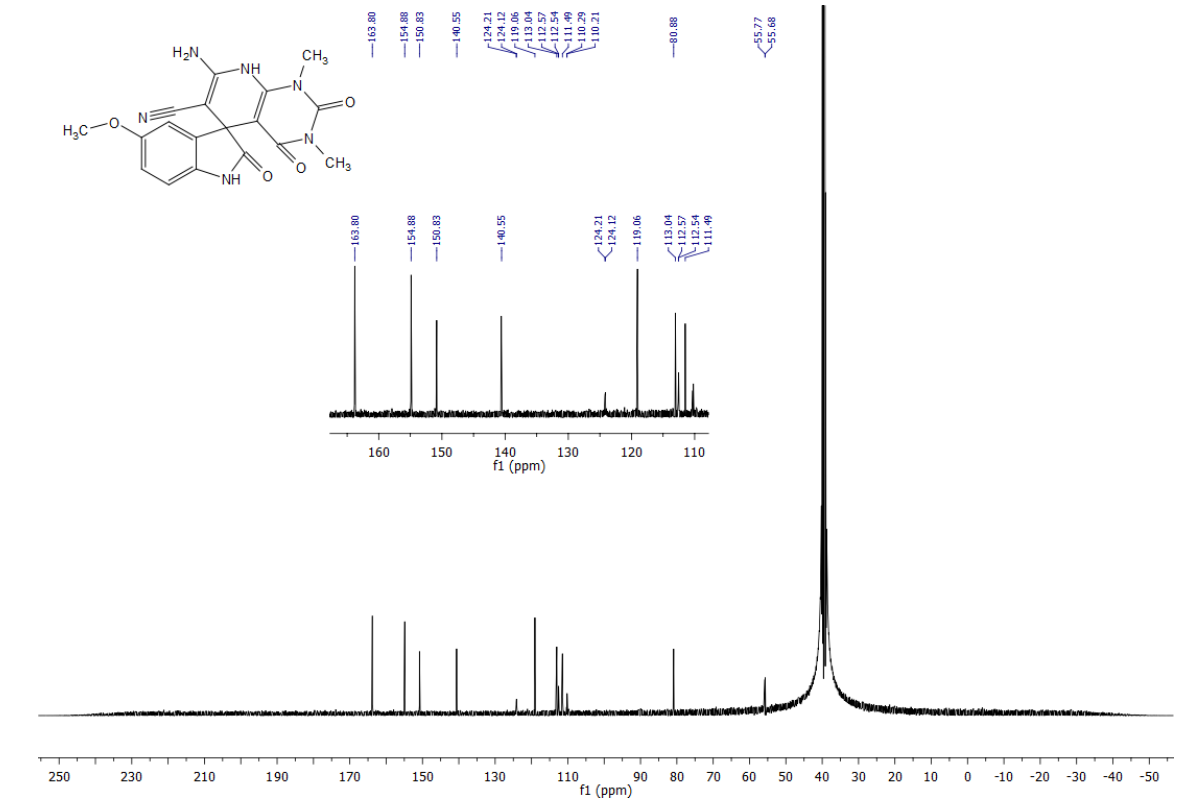

7'-Amino-5-chloro-1'-methyl-2,2',4'-trioxo-2',3',4',8'-tetrahydro-1'*H*-spiro[indoline-3,5'-pyrido[2,3-*d*]pyrimidine]-6'-carbonitrile (Table 5, entry 6e)

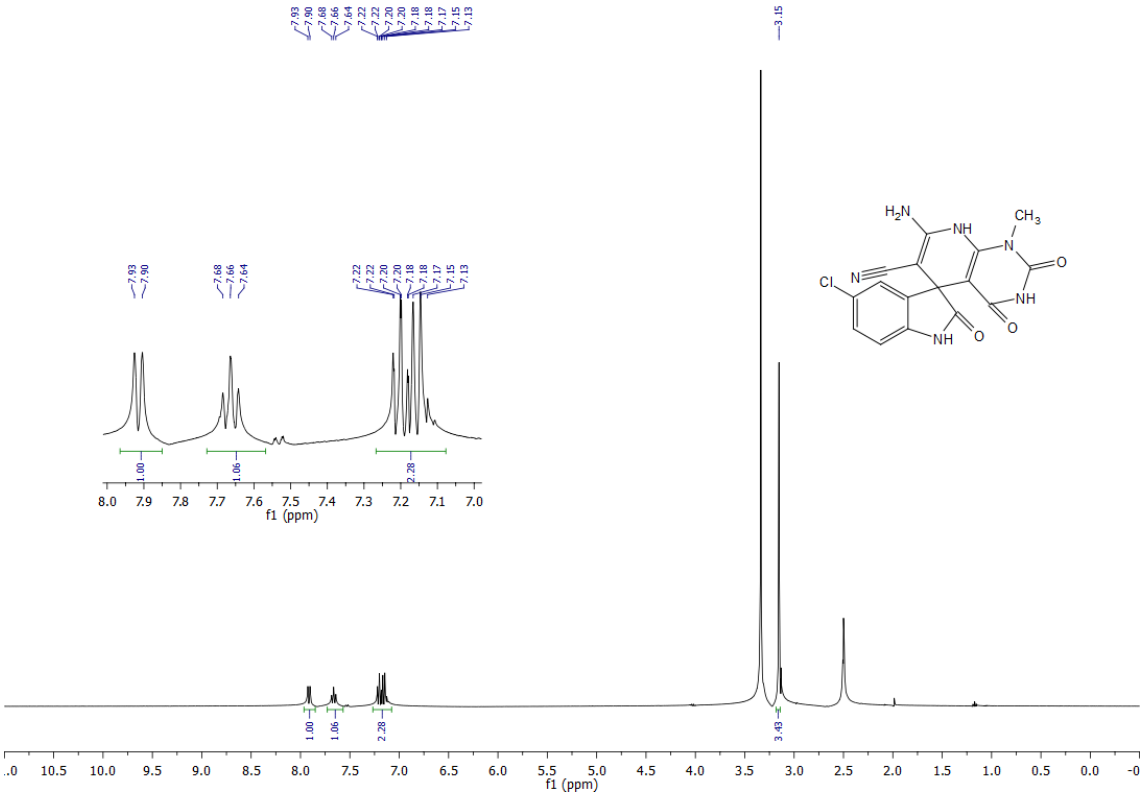

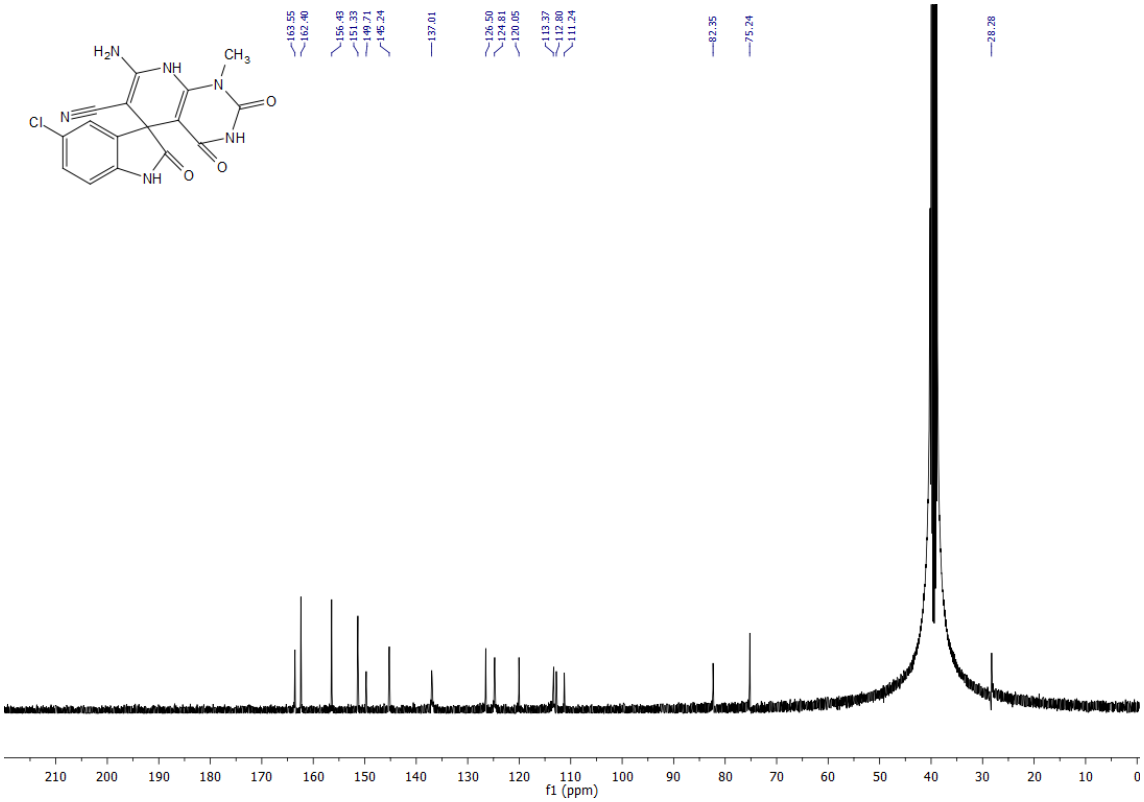

7'-Amino-5-chloro-1',3'-dimethyl-2,2',4'-trioxo-2',3',4',8'-tetrahydro-1'*H*-spiro[indoline-3,5'-pyrido[2,3-*d*]pyrimidine]-6'-carbonitrile (Table 5, entry 6f)

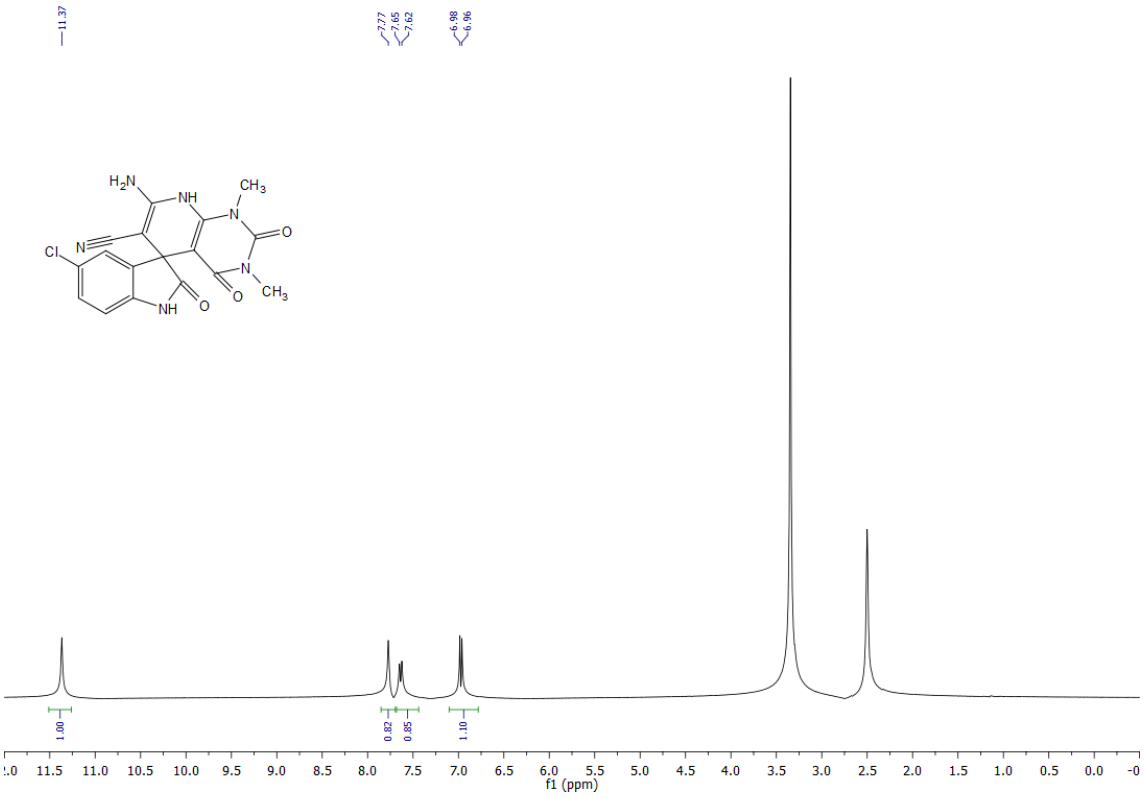

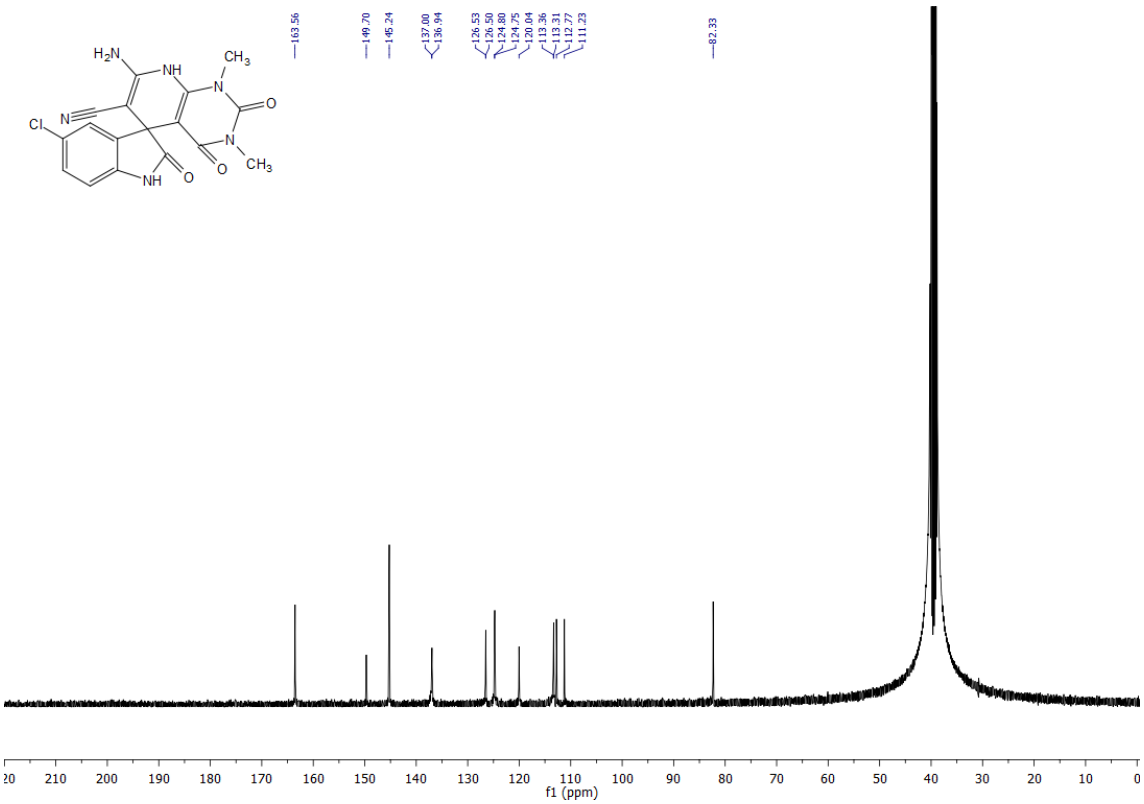

7'-Amino-1,1'-dimethyl-2,2',4'-trioxo-2',3',4',8'-tetrahydro-1'*H*-spiro[indoline-3,5'-pyrido[2,3-*d*]pyrimidine]-6'-carbonitrile (Table 5, entry 6g)

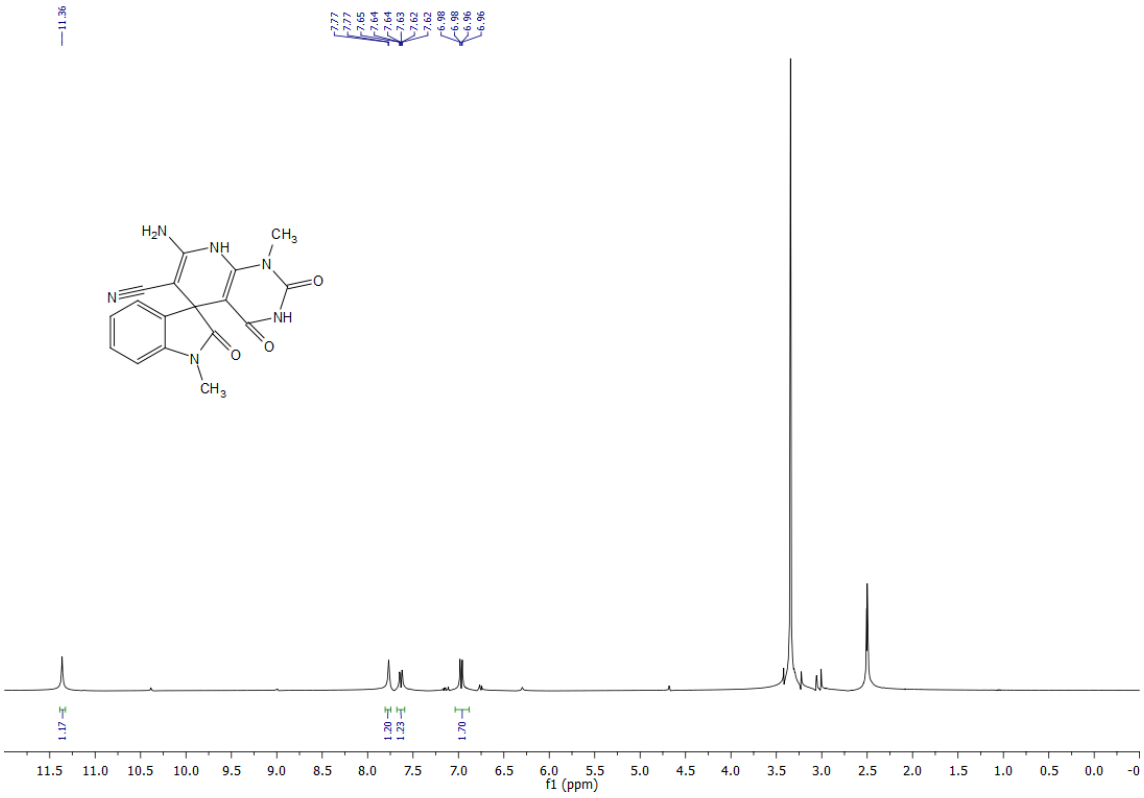

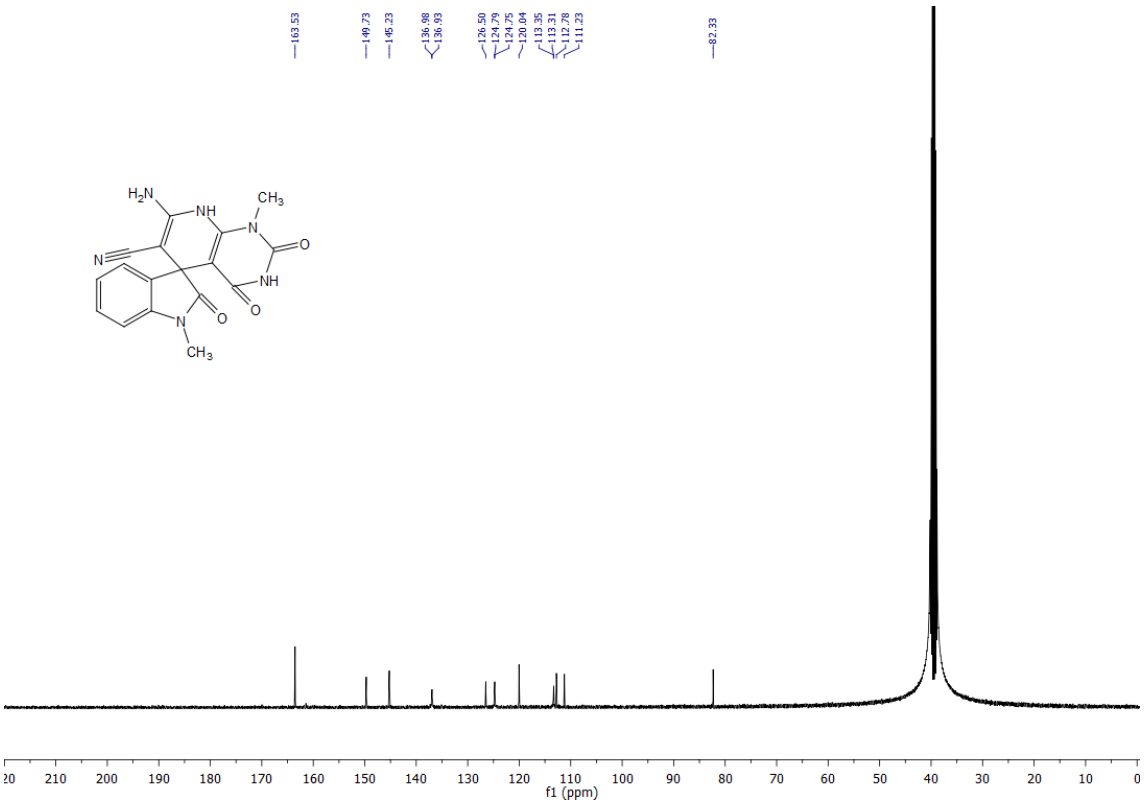

7'-Amino-1,1',3'-trimethyl-2,2',4'-trioxo-2',3',4',8'-tetrahydro-1'*H*-spiro[indoline-3,5'-pyrido[2,3-*d*]pyrimidine]-6'-carbonitrile (Table 5, entry 6h)

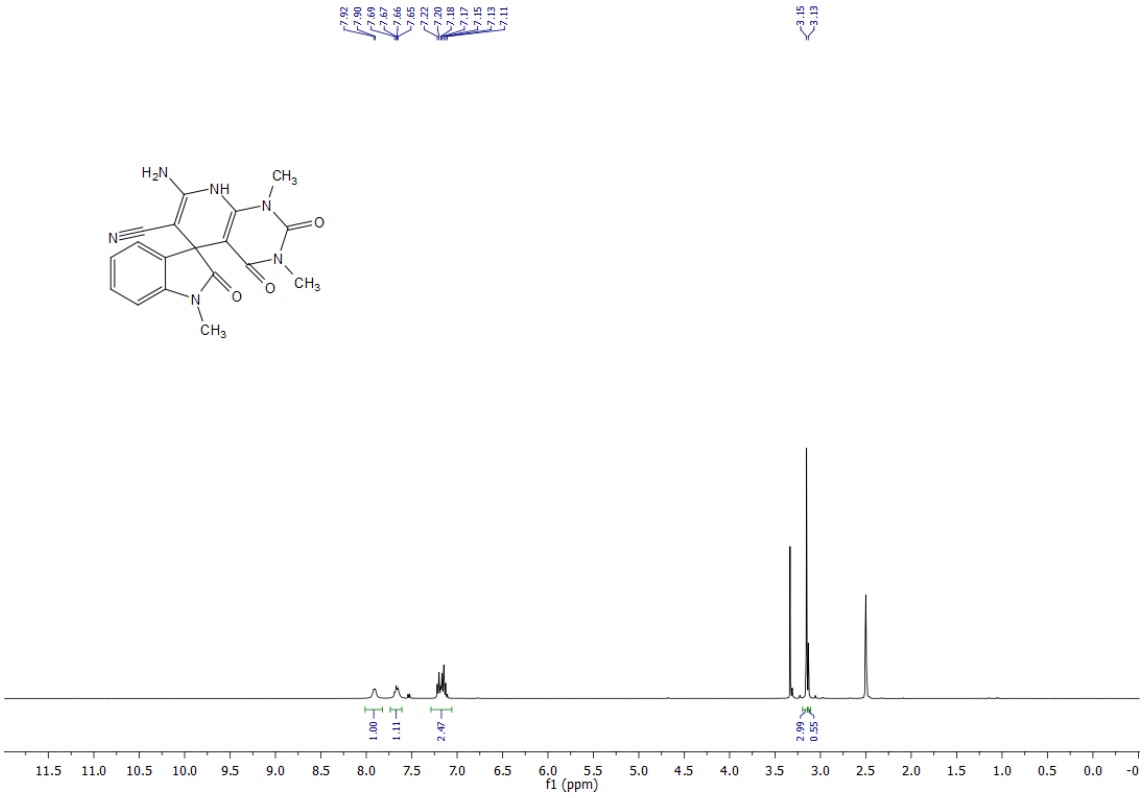

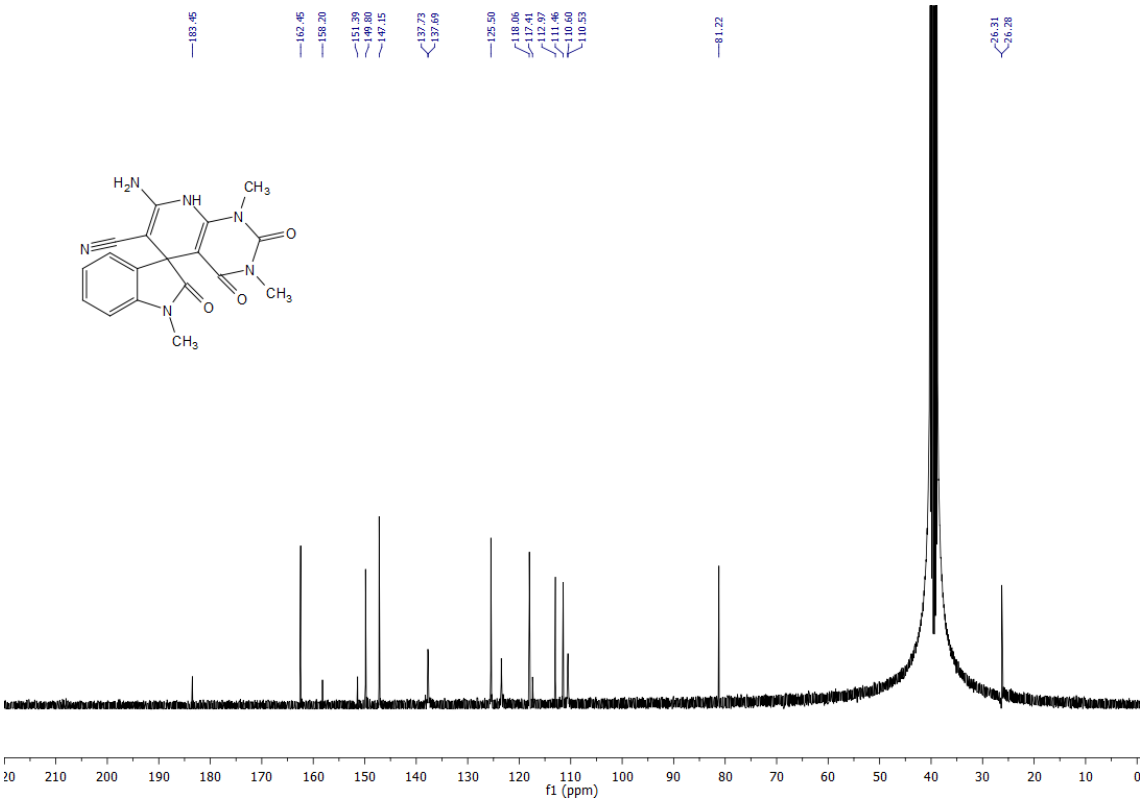

7'-Amino-1'-methyl-5-nitro-2,2',4'-trioxo-2',3',4',8'-tetrahydro-1'*H*-spiro[indoline-3,5'-pyrido[2,3-*d*]pyrimidine]-6'-carbonitrile (Table 5, entry 6i)

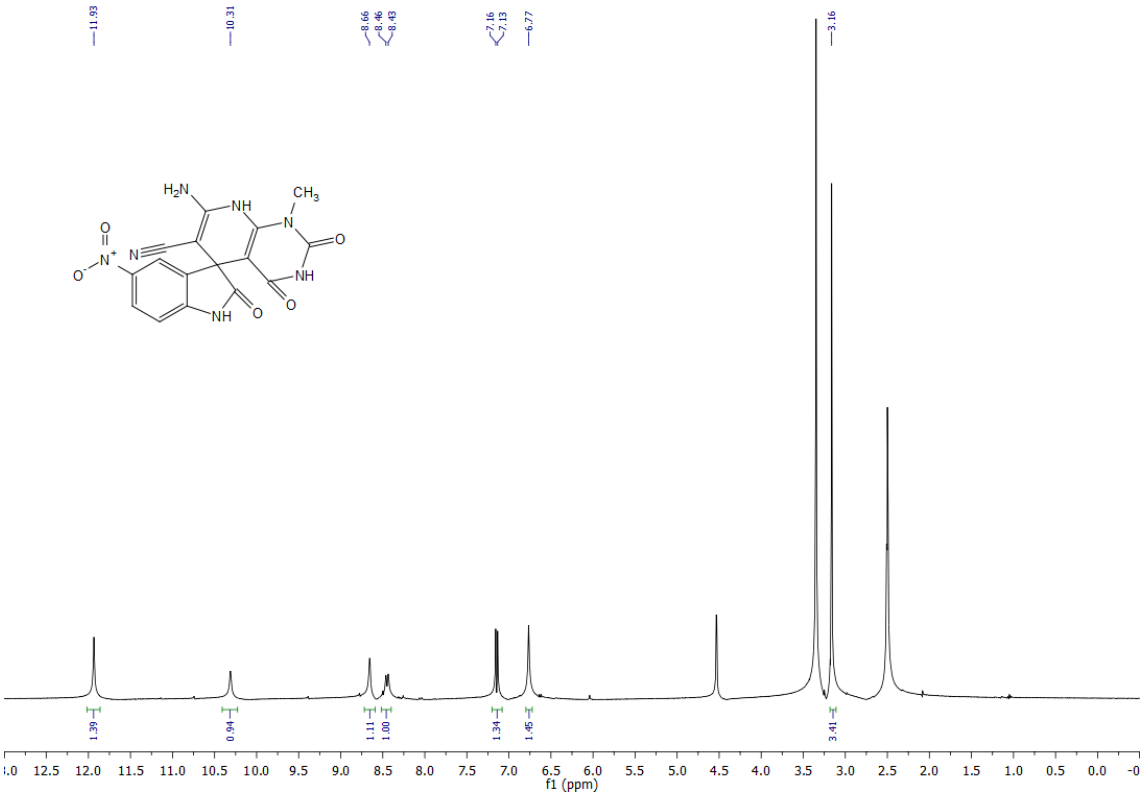

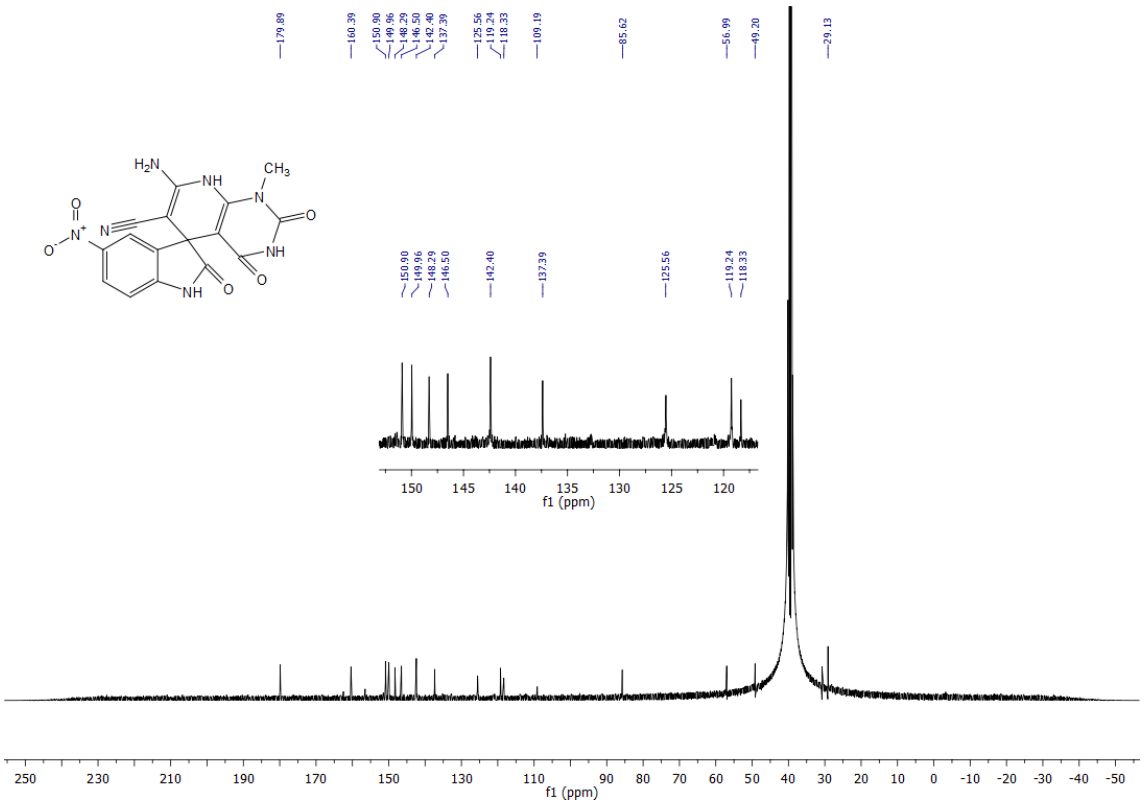

7'-Amino-1',3'-dimethyl-5-nitro-2,2',4'-trioxo-2',3',4',8'-tetrahydro-1'*H*-spiro[indoline-3,5'-pyrido[2,3-*d*]pyrimidine]-6'-carbonitrile (Table 5, entry 6j)

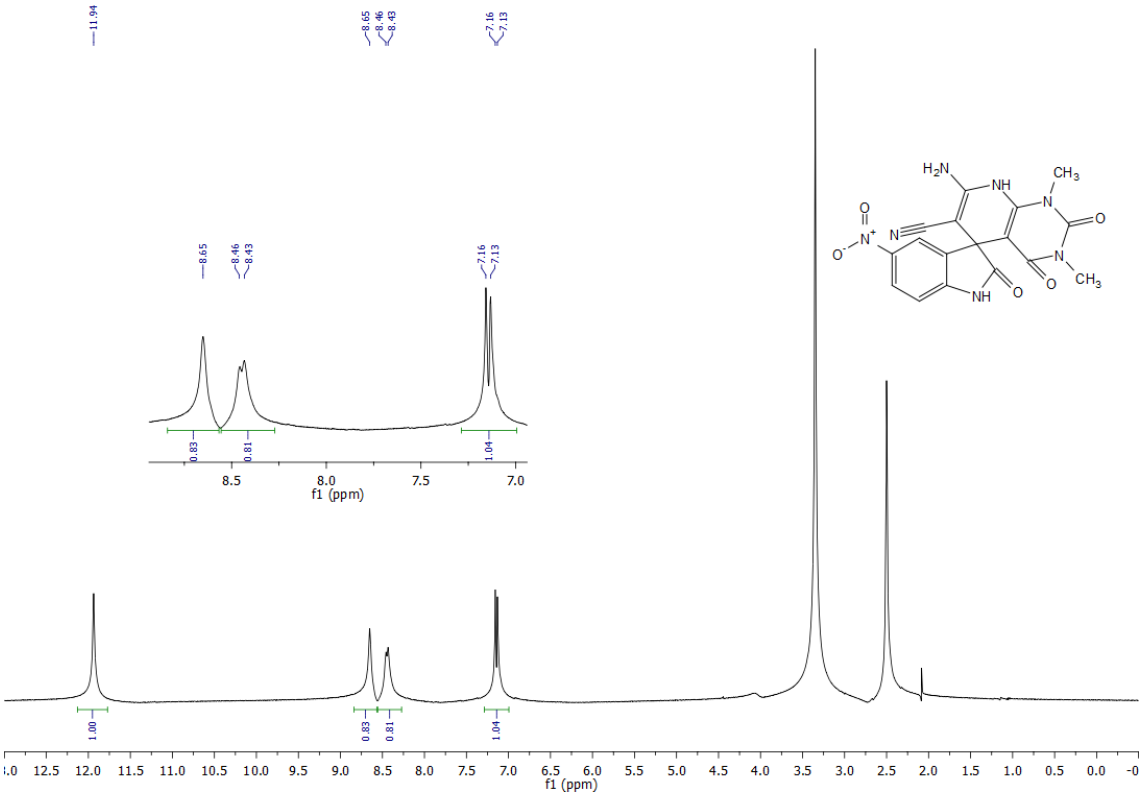

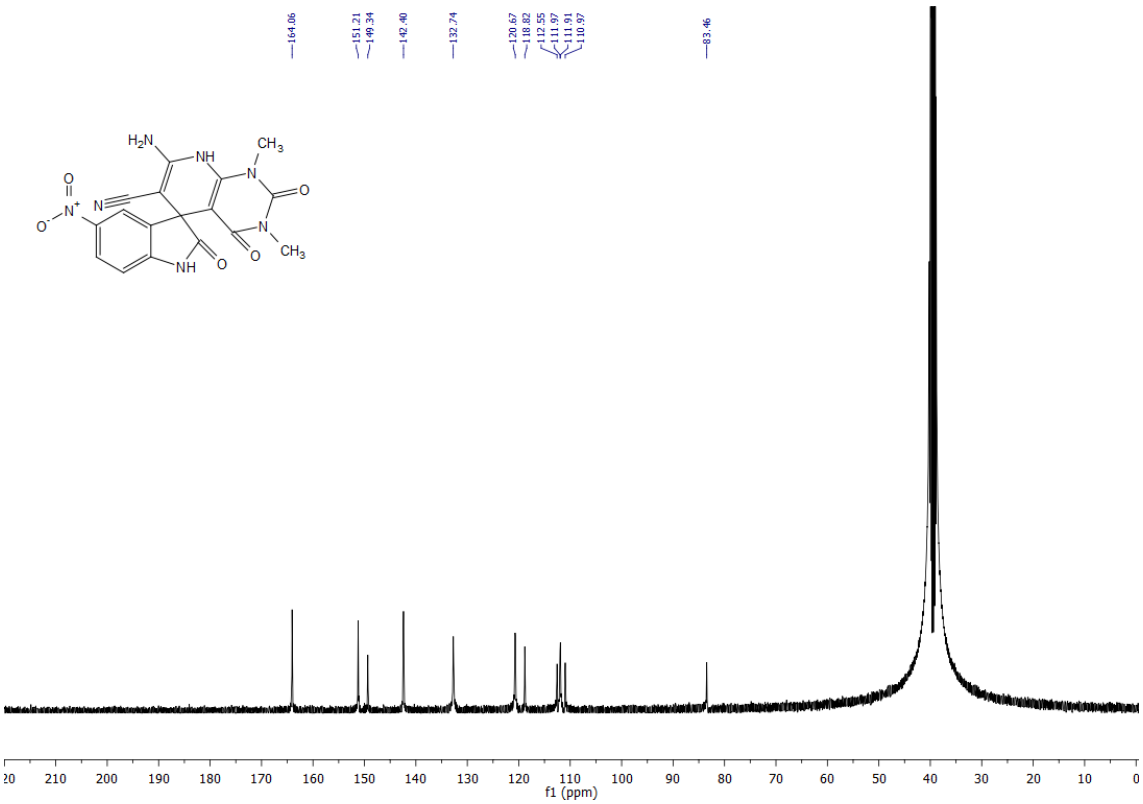

(10) Table S7. List of selected previous works

Sl. No.	Starting Material	Conditions	Product	Time (h)	Yield (%)	Reference
1	*N*-protected indoles	indole (0.5 mmol), $Cu(OAc)_2$ (0.025 mmol), TBHP (70% wt in H_2O, 1.0 mL), CH_3CN (3.0 mL), 50 °C	Isatin	12 h	0-90	3
2	*N*-protected indoles	indole (0.5 mmol), $Pd(OAc)_2$ (10 mol %), TBHP (70% wt in H_2O, 1.0 mL), CH_3CN (3.0 mL), 80 °C	Isatin	1 h	0-75	4
3	Indoles	indole (1 mmol), NIS (1.3 equiv.), IBX (3 equiv.), DMSO (2.0 mL), 25 °C	Isatin	3 h	73-89	5
4	Isatin, 5-amino-1,4-dimethyluracil, malonitrile	isatin (1 mmol), 5-amino-1,4-dimethyluracil (1 mmol), malonitrile (1 mmol), Fe_3O_4@SiO_2-TCTTheophylline (0.015, 0.85 mol%), H_2O (3 mL), reflux	Uracil-based spiroxindole	6-12 h	90-95	6

(11) NOE NMR spectrum of compound

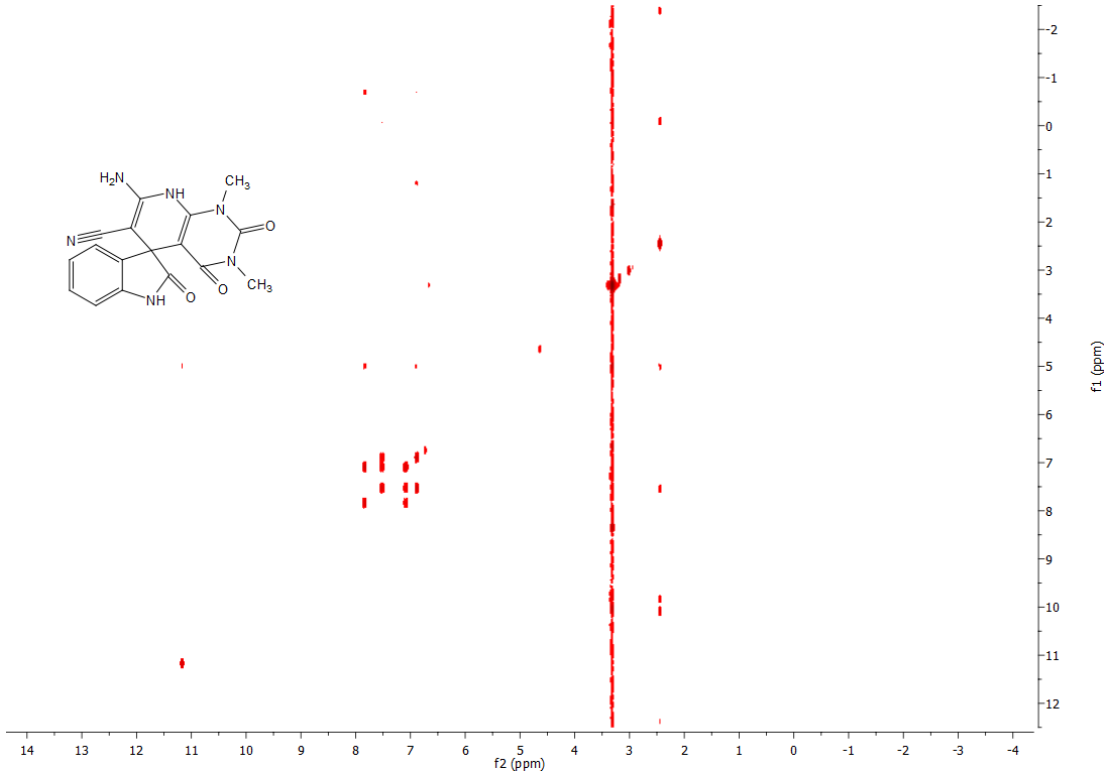

Figure S13. COSY NMR (in DMSO-d_6) of 7'-Amino-1',3'-dimethyl-2,2',4'-trioxo-2',3',4',8'-tetrahydro-1'*H*-spiro[indoline-3,5'-pyrido[2,3-*d*]pyrimidine]-6'-carbonitrile (Table 5, **entry 6b**)

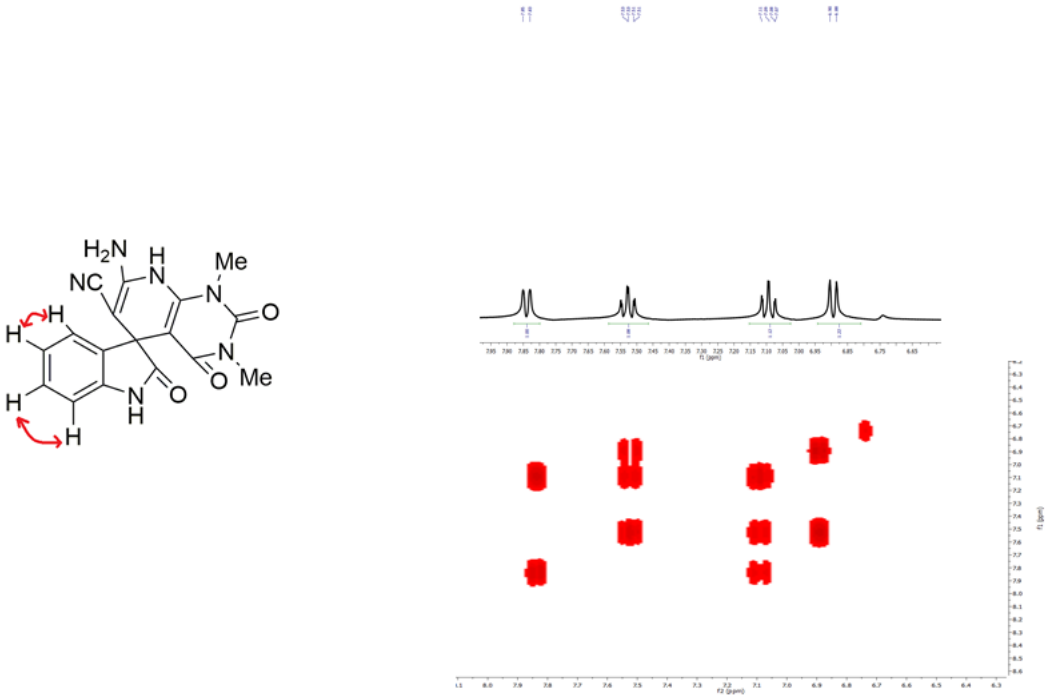

Figure S14. A representative $^{1}H–^{1}H$ COSY spectrum (in DMSO-d_6) of 7'-Amino-1',3'-dimethyl-2,2',4'-trioxo-2',3',4',8'-tetrahydro-1'*H*-spiro[indoline-3,5'-pyrido[2,3-*d*]pyrimidine]-6'-carbonitrile (Table 5, **entry 6b**)

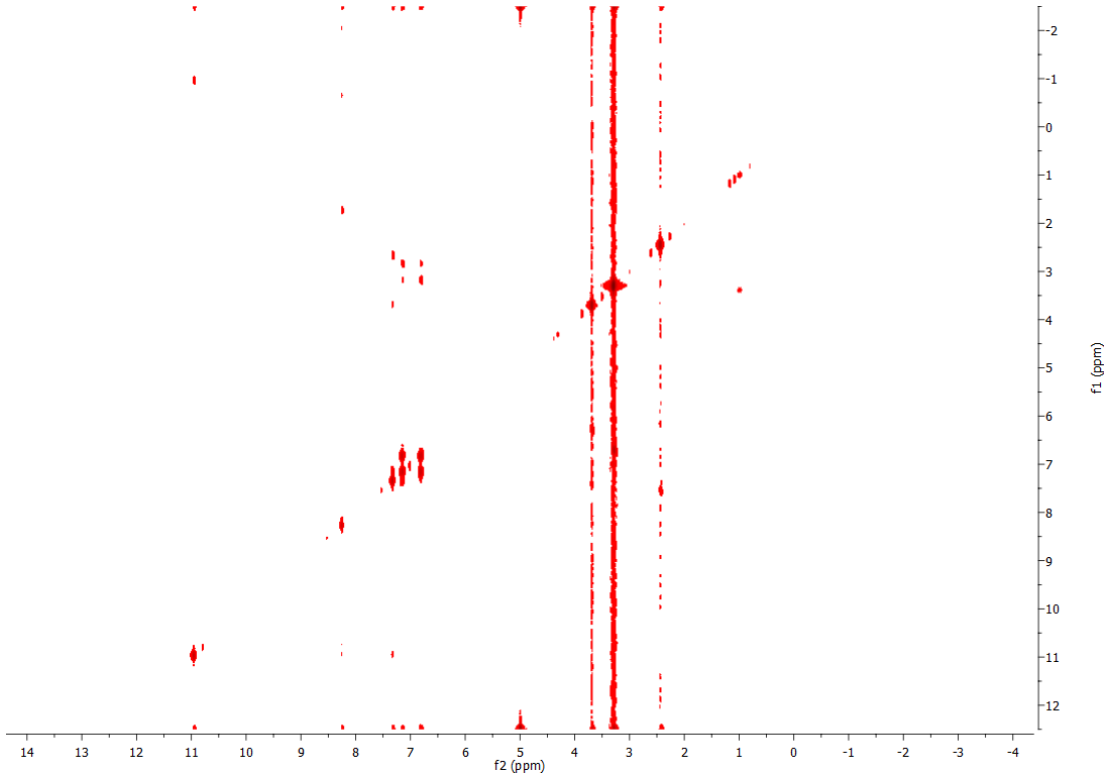

Figure S15. COSY NMR (in DMSO-d_6) of 7'-Amino-5-methoxy-1'-methyl-2,2',4'-trioxo-2',3',4',8'-tetrahydro-1'*H*-spiro[indoline-3,5'-pyrido[2,3-*d*]pyrimidine]-6'-carbonitrile(Table 5, **entry 6c**)

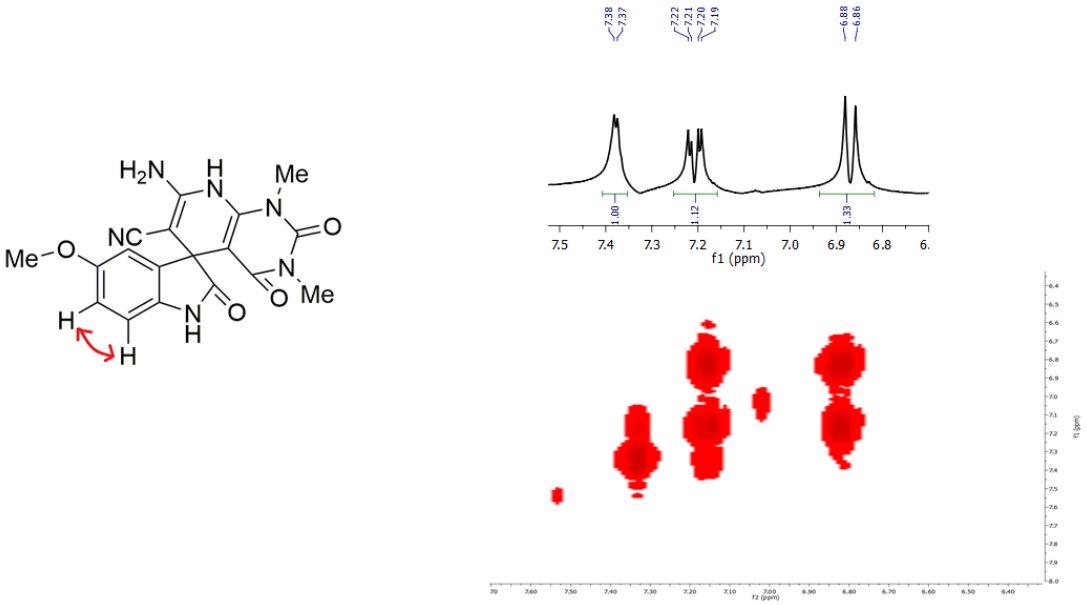

Figure 16. A representative $^{1}H–^{1}H$ COSY spectrum (in DMSO-d_6) of 7'-Amino-5-methoxy-1'-methyl-2,2',4'-trioxo-2',3',4',8'-tetrahydro-1'*H*-spiro[indoline-3,5'-pyrido[2,3-*d*]pyrimidine]-6'-carbonitrile (Table 5, **entry 6c**)

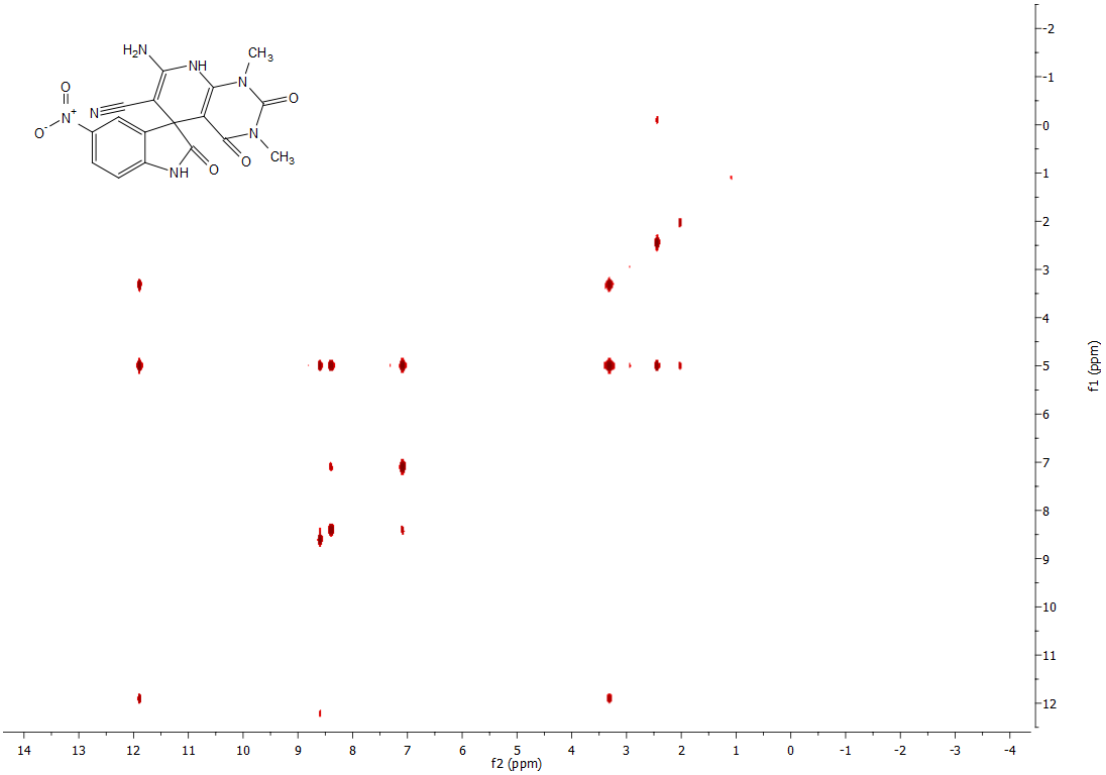

Figure 17. COSY NMR (in DMSO-d_6) of 7'-Amino-1',3'-dimethyl-5-nitro-2,2',4'-trioxo-2',3',4',8'-tetrahydro-1'*H*-spiro[indoline-3,5'-pyrido[2,3-*d*]pyrimidine]-6'-carbonitrile (Table 5, **entry 6j**)

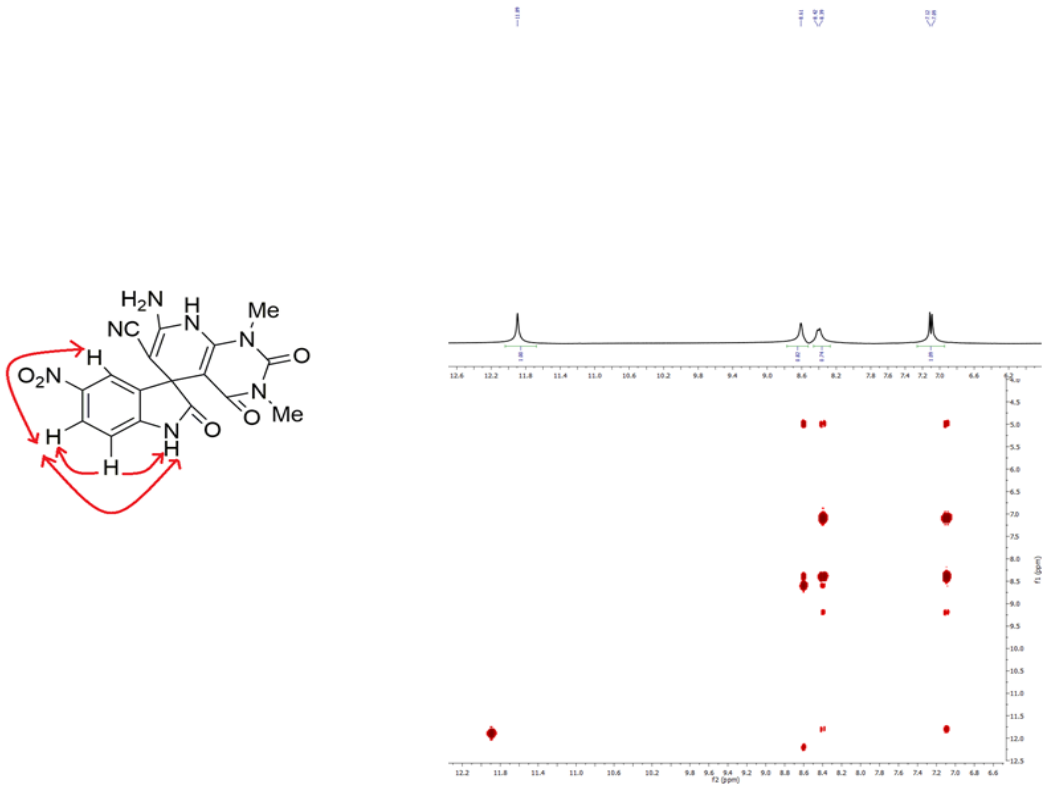

Figure 18. A representative $^{1}H–^{1}H$ COSY spectrum (in DMSO-*d*$_6$) of 7'-Amino-1',3'-dimethyl-5-nitro-2,2',4'-trioxo-2',3',4',8'-tetrahydro-1'*H*-spiro[indoline-3,5'-pyrido[2,3-*d*]pyrimidine]-6'-carbonitrile (Table 5, **entry 6j**)

(12) Calculation of Fe content in the catalyst Fe_3O_4/Au NPs-GO

0.2g $FeSO_4{\cdot}7H_2O$ solution in 110 mL was taken for preparation of Fe_3O_4/Au NPs.

(0.2/110 × 1000) g of $FeSO_4{\cdot}7H_2O$ in 1000 mL H_2O.

% of Fe in $FeSO_4{\cdot}7H_2O$ = 55.85/278.01 × 100 = 20.09%

20.09% of (0.2/110 ×1000) g of $FeSO_4$ = (0.2/110 ×1000) × (20.09/100) = 0.365 g

So, 0.365 g of Fe in 1000 mLH_2O.

Or (0.365 × 80)/1000 = 0.0292 g in 80 mL H_2O.

According to AAS of the decanted solution (supernatant) of Fe_3O_4/Au NPs-GO, concentration of Fe is 178.75 mg/L i.e. 0.17875 g/L.

Or (0.17875 × 80) mL = 14.3 mg or 0.0143 g in 80 mL H_2O.

So, concentration of Fe in the catalyst Fe_3O_4/Au NPs-GO = (Concentration of Fe taken for the reaction) – (Concentration of Fe in 80 mL of supernatant solution)

= (0.0292 – 0.0143) g

= 0.0149 g in 250 mg catalyst

Thus, 0.1 mg of catalyst will contain = (0.0149 × 0.1)/250 g

= 0.000006 g Fe

= 0.006 mg Fe

For calculating the mol%, the formula is shown below,

Reactant (g)/ Molar mass of the reactant (g/mol) ×mol% × Catalyst molar mass (g/mol)

= Weight of catalyst (g)

for which the molar mass of the catalyst is to be known. As the molar mass of the support (graphene oxide) is not able to be defined with respect to atomic mass, so the weight of the catalyst is taken as reference for the reaction conditions in application of the catalyst in synthesis of indolinones and spirooxindoles.

(13) References

[1] W. S. Hummers, R. E. Offeman, *J. Am. Chem. Soc.*, 1958, **80**, 1339

[2] S. Thakur, N. Karak, *RSC Adv.*, 2013, **3**, 9476-9482.

[3] J. Luo, Y. Zhao, X. Xu, J. Zheng, H. Liang, *Tetrahedron Lett.*, 2017, **58**, 4591-4594.

[4] J. Luo, S. Gao, Y. Ma, G. Ge, *Synlett*, 2018, **29**, 969-973.

[5] A. Chandra, N. R. Yadav, J. N. Moorthy, *Tetrahedron*, 2019, **75**, 2169-2174.

[6] M. Esmaeilpour, A. R. Sardarian, H. Firouzabadi, *ChemistrySelect*, 2018, **3**, 9236-9248.